Published in : Journal of Experimental Botany (2023), vol. 74, n°15, pp. 4540-4558

DOI: 10.1093/jxb/erad170

Status : Postprint (Author's version)

RESEARCH PAPER

ACCLIMATION STRATEGIES OF THE GREEN ALGA *CHLORELLA VULGARIS* TO DIFFERENT LIGHT REGIMES REVEALED BY PHYSIOLOGICAL AND COMPARATIVE PROTEOMIC ANALYSES

Michela Cecchin[1], Jovan Simicevic[2], Louise Chaput[2], Manuel Hernandez Gil[2], Laura Girolomoni[1], Stefano Cazzaniga[1], Claire Remacle[3], Julia Hoeng[2], Nikolai V. Ivanov[2], Bjoern Titz[2] and Matteo Ballottari[1,*]

[1]*Dipartimento di Biotecnologie, Università di Verona, Strada Le Grazie 15, 37134 Verona, Italy*

[2]*PMI R&D, Philip Morris Products S.A., Quai Jeanrenaud 5, 2000 Neuchâtel, Switzerland*

[3]*Genetics and Physiology of Microalgae, InBios/Phytosystems Research Unit, University of Liège, 4000 Liège, Belgium*

** Correspondence: matteo.ballottari@univr.it*

ABSTRACT

Acclimation to different light regimes is at the basis of survival for photosynthetic organisms, regardless of their evolutionary origin. Previous research efforts largely

Published in : Journal of Experimental Botany (2023), vol. 74, n°15, pp. 4540-4558

DOI: 10.1093/jxb/erad170

Status : Postprint (Author's version)

focused on acclimation events occurring at the level of the photosynthetic apparatus and often highlighted species-specific mechanisms. Here, we investigated the consequences of acclimation to different irradiances in *Chlorella vulgaris*, a green alga that is one of the most promising species for industrial application, focusing on both photosynthetic and mitochondrial activities. Moreover, proteomic analysis of cells acclimated to high light (HL) or low light (LL) allowed identification of the main targets of acclimation in terms of differentially expressed proteins. The results obtained demonstrate photosynthetic adaptation to HL versus LL that was only partially consistent with previous findings in *Chlamydomonas reinhardtii*, a model organism for green algae, but in many cases similar to vascular plant acclimation events. Increased mitochondrial respiration measured in HL-acclimated cells mainly relied on alternative oxidative pathway dissipating the excessive reducing power produced due to enhanced carbon flow. Finally, proteins involved in cell metabolism, intracellular transport, gene expression, and signaling—including a heliorhodopsin homolog—were identified as strongly differentially expressed in HL versus LL, suggesting their key roles in acclimation to different light regimes.

KEYWORDS: Abiotic stress, carotenoids, *Chlorella vulgaris*, microalgae, photosynthesis, proteomics.

Published in : Journal of Experimental Botany (2023), vol. 74, n°15, pp. 4540-4558

DOI: 10.1093/jxb/erad170

Status : Postprint (Author's version)

ABBREVIATIONS: ABC1K1, activity of bc1 complex kinase 1; ACS, acetyl-CoA synthase; AOX, alternative oxidase; CBB, Calvin–Benson–Bassham; Chl, chlorophyll; DBMIB, 2,5-dibromo-6-isopropyl-3-methyl-1,4-benzoquinone; DCMU, 3-(3,4-dichlorophenyl)-1,1-dimethylurea; ECS, electrochemical shift; FDR, false discovery rate; GO, Gene Ontology; HL, high light; LHCSR, light-harvesting complex stress related; LL, low light; LRR, leucine-rich repeat; NPQ, non-photochemical quenching; PAT, phosphate acetyltransferase; Pmax, maximum light-dependent net oxygen evolution rate; PTOX, Plastid Terminal Oxidase; qL, fraction of open reaction centers in PSII; SHAM, salicylhydroxamic acid; TCA, tricarboxylic acid,

Introduction

Photosynthesis is the metabolic process by which light energy into organic molecules, as sugars. In eukaryotic photosynthetic is harvested and converted into chemical energy to fix CO_2 organisms, PSI and PSII are the pigment-binding complexes located in the thylakoid membranes that harvest photons and use the excitation energy to generate electron transport from water to NADPH; this electron transport is coupled with proton transport that generates an electrochemical gradient across thylakoid membranes, enabling ATP biosynthesis. The Calvin–Benson–Bassham (CBB) cycle is the subsequent

Published in : Journal of Experimental Botany (2023), vol. 74, n°15, pp. 4540-4558

DOI: 10.1093/jxb/erad170

Status : Postprint (Author's version)

metabolic process occurring in the stroma where ATP and NADPH are consumed to fix CO_2. Among photosynthetic organisms, unicellular microalgae raised interest due to the possibility to cultivate them in artificial systems in industrial environments to exploit their photosynthetic capability to fix CO_2 into bioproducts of interest including food additives, proteins, lipids, antioxidants, biostimulants, and possibly biofuels (Chisti, 2008; Camacho *et al.*, 2019; Koyande *et al.*, 2019; Rosch *et al.*, 2019; Rani *et al.*, 2021). Several microalgae species were considered for industrial application, such as *Chlorella* species, which are characterized by fast growth and high resistance to biotic and abiotic stresses (Blanc *et al.*, 2010; Juneja *et al.*, 2016; Treves *et al.*, 2016; Zuniga *et al.*, 2016; Ananyev *et al.*, 2017; Sarayloo *et al.*, 2017; Arriola *et al.*, 2018; Niccolai *et al.*, 2019; Sathasivam *et al.*, 2019). Indeed, some *Chlorella* species are already on the market as food and feed supplements (Lum *et al.*, 2013). *Chlorella vulgaris* is one of the few microalgae species approved as novel food for human consumption (Bernaerts *et al.*, 2019).

Microalgae photosynthetic efficiency and productivity are strictly dependent on their capacity to adapt and acclimate to the conditions of growth where irradiance, temperature, CO_2, and nutrient availability are among the key parameters influencing cell growth (Vecchi *et al.*, 2020). The consequences of growing at different light intensities were investigated in depth in several microalgae species in previous works: the

Published in : Journal of Experimental Botany (2023), vol. 74, n°15, pp. 4540-4558

DOI: 10.1093/jxb/erad170

Status : Postprint (Author's version)

chlorophyll (Chl) content per cell and Chl to carotenoid ratio are generally reduced for different microalgae species grown in high light (HL) compared with cells acclimated to low light (LL) (Bonente *et al.*, 2012; Simionato *et al.*, 2011). Moreover, the light-harvesting capacity, or functional 'antenna size', of PSII, measured from the Chl *a* fluorescence induction curve in the presence of a PSII inhibitor, or estimated from the Chl *a*/*b* ratio, was reported to be reduced in several species such as *Dunaliella salina*, *Dunaliella viridis* (Smith *et al.*, 1990; Gordillo *et al.*, 2001), and diatoms (Lavaud *et al.*, 2004) upon acclimation to HL. In contrast, in the case of the model organism for green algae, *Chlamydomonas reinhardtii*, and in *Nannochloropsis gaditana*, similar functional antenna sizes were measured in cells grown at low or high irradiance (Simionato *et al.*, 2011; Bonente *et al.*, 2012). Cells grown in HL conditions are also generally characterized by an increased capability to induce photoprotective mechanisms as thermal dissipation of the light absorbed (or non-photochemical quenching, NPQ) as reported in the case of *C. reinhardtii* (Peers *et al.*, 2009), diatoms (Zhu and Green, 2010; Lepetit *et al.*, 2012), and *Nannochloropsis* (Chukhutsina *et al.*, 2017). Regulation of CBB enzyme accumulation and activity was also reported to have a key role in acclimation to HL, with a general increased capacity for carbon fixation in cells acclimated to high irradiance (Bonente *et al.*, 2012). It is important to note that in eukaryotic photosynthetic organisms as in microalgae, photosynthetic metabolism is coupled with mitochondrial metabolism (Johnson and

Published in : Journal of Experimental Botany (2023), vol. 74, n°15, pp. 4540-4558

DOI: 10.1093/jxb/erad170

Status : Postprint (Author's version)

Alric, 2013; Bailleul *et al.*, 2015; Uhmeyer *et al.*, 2017), where organic molecules are oxidized to CO_2, producing reducing power that can in turn be used to produce ATP. The mitochondrial electron transport chain, also known as the cytochrome pathway, includes an ATP synthase complex (complex V) and four oxidoreductase complexes that oxidize the reducing power and produce ATP by an electrochemical gradient that is formed across the membrane. In addition, an alternative oxidase (AOX) might directly couple ubiquinol oxidation with the reduction of O_2 to H_2O, serving as an alternative route that bypasses the electron transport chain, thus dramatically reducing the energy (ATP) yield. In plants, AOX was reported to have a role in respiratory chain protection mechanisms by preventing saturation of the electron carriers (Boekema and Braun, 2007; Vanlerberghe, 2013). An additional alternative oxidase, called PTOX (Plastid Terminal Oxidase), was characterized in the chloroplast as being involved in chlororespiration transferring electrons from the plastoquinone pool to oxygen (Arnon *et al.*, 1981; Bennoun, 1982; Rumeau *et al.*, 2007; Kedem *et al.*, 2021). PTOX activity has been previously reported to prevent electron transport chain saturation (Niyogi, 2000; Kedem *et al.*, 2021), but at same time its activity has been shown to be crucial for carotenogenesis (Shahbazi *et al.*, 2007; Li *et al.*, 2010). It is important to note that crosstalk between plastids and mitochondria was proposed in several microalgae species, where the activity of one of the two organelles influences the redox state of the

Published in : Journal of Experimental Botany (2023), vol. 74, n°15, pp. 4540-4558

DOI: 10.1093/jxb/erad170

Status : Postprint (Author's version)

other (Bailleul *et al.*, 2015; Uhmeyer *et al.*, 2017; Burlacot *et al.*, 2019; Cecchin *et al.*, 2021b). In this context, the impact of mitochondrial activity in HL acclimation in microalgae has not been fully elucidated.

In this work, we investigated the consequences of acclimation at high or low irradiances in *C. vulgaris* with a focus on photosynthetic and mitochondrial activities. Moreover, proteomic analysis of cells acclimated to HL or LL allowed us to identify the main target of acclimation in terms of variable protein expression, suggesting possible targets for future biotechnological modifications.

Materials and methods

Chlorella vulgaris cultivation

Chlorella vulgaris strain 211-11p (Cecchin *et al.*, 2019) was obtained from the Culture Collection of Algae at Goettingen University. LL and HL acclimation was induced by growing *C. vulgaris* cells in photoautotrophy in BG-11 medium (Allen and Stanier, 1968) at 25 °C (Serra-Maia *et al.*, 2016) in flasks at 70 µmol m^{-2} s^{-1} or 850 µmol m^{-2} s^{-1} white light irradiation. No additional inorganic carbon was supplied, and a rotary shaker (150 rpm) was used to prevent cell sedimentation and induce gas exchange. The cell cultures were

Published in : Journal of Experimental Botany (2023), vol. 74, n°15, pp. 4540-4558

DOI: 10.1093/jxb/erad170

Status : Postprint (Author's version)

exposed to light from the bottom of the flask, and the light path (from the bottom to the top of the culture) was 1 cm. The light gradient at which the cells were exposed during growth was calculated from the pigment concentration in the cultures and their transmittance spectra (Supplementary Fig. S1). The cells grown in LL and HL conditions were refreshed at least 10 times, diluting the cells to pre-exponential phase before the experiments. Sampling for physiological measurements and for proteomic analysis was done during the exponential phase for at least three different biological replicates grown at the same time. At the end of the growth curve, the dry weight determination was performed: the cell culture was harvested by centrifugation at 4500 *g* for 5 min at 20 °C, freeze-dried for 48 h, and then net dry weight was calculated. Protein concentration was determined by bicinchoninic acid (BCA) protein assay (Thermo Fisher Scientific, Waltham, MA, USA).

Photosynthetic parameters

Photosynthetic parameters such as maximum photochemical efficiency of PSII (ΦPSII), fraction of open reaction centers in PSII (qL), electron transport rate (ETR), and NPQ were measured with a DUAL-PAM-100 fluorometer (Heinz–Walz, Effeltrich, Germany) at room temperature in a 1 × 1 cm cuvette mixed by magnetic stirring (Baker, 2008). PSII functional antenna size was estimated from the fast Chl fluorescence induction kinetics

Published in : Journal of Experimental Botany (2023), vol. 74, n°15, pp. 4540-4558

DOI: 10.1093/jxb/erad170

Status : Postprint (Author's version)

with a DUAL-PAM-100 fluorometer after induction with a red light of 11 µmol photons m^{-2} s^{-1} on dark-adapted cells (~2 × 10^6 cells ml^{-1}) incubated with 50 µM DCMU [3-(3,4-dichlorophenyl)1,1-dimethylurea]. The reciprocal of time corresponding to two-thirds of the fluorescence rise (τ2/3) was taken as a measure of the PSII functional antenna size (Malkin *et al.*, 1981). The 77K fluorescence emission spectra were acquired with a charge-coupled device spectrophotometer (JBeamBio, La Rochelle, France) as previously described (Allorent *et al.*, 2013). State transitions were measured on whole cells induced to state 1 or state 2 as previously described (Fleischmann *et al.*, 1999). The reduction rate of NAD(P)H was determined with the NADPH/9-AA module of the DUAL-PAM 101 using 1400 µmol photons m^{-2} s^{-1} as actinic light (Schreiber and Klughammer, 2009; Cecchin *et al.*, 2021b): NAD(P) H formation was analyzed following the fluorescence emission in the 420–580 nm range upon excitation at 365 nm. The proton motive force upon exposure to different light intensities was measured as the electrochemical shift (ECS) with MultispeQ v2.0 (PhotosynQ, East Lansing, MI, USA) according to Kuhlgert *et al.* (2016) and normalized to the Chl content of the sample. PSI functional antenna size was measured in thylakoids (300 µg ml^{-1} Chl concentration) obtained from acclimated cells with the DUAL-PAM-100 in the presence of DCMU and DBMIB (2,5-dibromo-6-isopropyl-3-methyl-1,4-benzoquinone) following transient absorption at 830 nm upon exposure to actinic

Published in : Journal of Experimental Botany (2023), vol. 74, n°15, pp. 4540-4558

DOI: 10.1093/jxb/erad170

Status : Postprint (Author's version)

light (11 µmol photons m^{-2} s^{-1}). Maximum P700 activity was measured as described in Cecchin *et al.* (2021b).

Pigment analysis

Pigments were extracted with 100% DMSO at 60 °C in dark conditions and measured with a JASCO V-550 UV/VIS spectrophotometer (Halifax, NS, Canada). HPLC analysis was performed as described in Perozeni *et al.* (2020).

Oxygen evolution and mitochondrial respiration

Oxygen evolution rates and mitochondrial respiration were measured at 25 °C with a Clark-type O_2 electrode (Hansatech, King's Lynn, Norfolk, UK), as described previously (Cecchin *et al.*, 2021b). $NaHCO_3$ was supplied before oxygen evolution measurement at 5 mM concentration. The individual contributions of the alternative and cytochrome (complex III) pathways in mitochondrial respiration were estimated by inhibiting them with SHAM (salicylhydroxamic acid) and myxothiazol inhibitors, respectively; the concentrations adopted, 2 mM and 5 µM, respectively, were chosen according to previous results in the same species (Cecchin *et al.*, 2021b). Respiration was first measured in the absence of inhibitors (total dark respiration) before alternative respiration was inhibited by adding SHAM. Cytochrome-dependent respiration was then inhibited using myxothiazol, and residual respiration was determined in relation to the

Published in : Journal of Experimental Botany (2023), vol. 74, n°15, pp. 4540-4558

DOI: 10.1093/jxb/erad170

Status : Postprint (Author's version)

uninhibited state. The contribution of alternative respiration was determined by reversing the order of inhibitor addition (myxothiazol followed by SHAM) (Bailleul *et al.*, 2015).

SDS–PAGE and western blot analysis

SDS–PAGE and immunoblotting were performed as described in Bonente *et al.* (2011). The following antibodies, α-RbcL AS03 037, α-PsaA AS06 172, and α-PsbC (CP43) AS11 1787, were obtained from Agrisera (Vannas, Sweden). Samples were compared only when loaded on the same gel.

Subcellular localization prediction

Subcellular localization prediction was performed with the PredAlgo tool (Tardif *et al.*, 2012).

Proteomic analysis

Chlorella vulgaris sample cell disruption was performed utilizing a CP02 cryoPREP Automated Dry Pulverizer (Covaris, Woburn, MA, USA); total protein was extracted with the ReadyPrep Protein Extraction Kit (Bio-Rad, Hercules, CA, USA) and a Tissue Lyser II system (Qiagen, Hilden, Germany). Samples were then centrifuged for 5 min at 16 000 *g*, and the supernatants (400 µl) were transferred to new tubes. Proteins were precipitated

Published in : Journal of Experimental Botany (2023), vol. 74, n°15, pp. 4540-4558

DOI: 10.1093/jxb/erad170

Status : Postprint (Author's version)

by separately adding four volumes of acetone to one volume of each protein extract, vortexed, and precipitated overnight at –20 °C. The next day, individual tubes were centrifuged for 30 min at 10 °C at 16 000 *g*. The supernatants were removed, then one volume of prechilled acetone was added to each tube. The tubes were centrifuged one more time, and the previous step was repeated. The supernatants were again discarded, and the protein pellets were dried using a speed vacuum for <1 min. The dried protein pellets were separately resuspended in 200 µl of resuspension buffer [1 M urea, 0.5 M triethylammonium bicarbonate (TEAB), 0.1% SDS], vortexed, and centrifuged at 16 000 *g* for 25 s. The samples were sonicated for 30 s then centrifuged for 1 min at 16 000 *g* before the supernatants were collected. Protein amounts were measured with the Quick Start Bradford Protein Assay (Bio-Rad) utilizing BSA as the standard. Protein concentrations were normalized to 1 µg μl^{-1} in resuspension buffer in a final volume of 30 µl. Protein reduction, alkylation, digestion, and purification were performed utilizing the Preomics iST protein sample preparation for the LC-MS kit (Preomics, Planegg/ Martinsried, Germany) according to the manufacturer's instructions. The resulting purified peptides were resuspended in 30 µl of nanoLC-Buffer A (5% acetonitrile, 0.2% formic acid). Samples were analyzed in protein profiling mode using an EASY-nLC 1200 liquid chromatography system (Thermo Fisher Scientific) coupled to a Q-Exactive HF mass spectrometer (Thermo Fisher Scientific). Prior to MS measurements, samples were

Published in : Journal of Experimental Botany (2023), vol. 74, n°15, pp. 4540-4558

DOI: 10.1093/jxb/erad170

Status : Postprint (Author's version)

diluted 2-fold with nanoLC-Buffer A spiked with 1/10 iRT peptides (Biognosys, Schlieren, Switzerland); 2 µl of sample were injected and fractionated in a 50 cm long C18RP RSLC ES803 Easyspray column (Thermo Fisher Scientific) at a flow rate of 200 nl min^{-1} with a 200 min gradient from nanoLC buffer A to 40% acetonitrile, 0.2% formic acid.

A *C. vulgaris* protein sequence database was derived from our own sequencing effort (Cecchin *et al.*, 2019) and entries were annotated based on species sequence orthology. Raw MS data were processed using the Spectronaut software package (Version 15, Biognosys) against the above-mentioned protein database in directDIA mode. A dataset containing potential protein contaminants and sequences of iRT peptides (Biognosys) used for retention time normalization was utilized for Spectronaut data processing. Further data processing was performed in the R statistical environment. For each protein, the obtained quantification values were summed for quantified peptides and charge states. Proteins with missing values in <50% of the samples were retained. Data were log-transformed and normalized for equal medians across all samples. For the detection of differentially expressed proteins, a linear model was fitted for the treatment and control groups, and *P*-values from moderated *t*-statistics were calculated with the empirical Bayes approach (Gentleman *et al.*, 2004). The Benjamini–Hochberg false discovery rate (FDR) method was used to correct for multiple hypotheses testing.

Published in : Journal of Experimental Botany (2023), vol. 74, n°15, pp. 4540-4558

DOI: 10.1093/jxb/erad170

Status : Postprint (Author's version)

Gene set enrichment analysis (GSEA) was performed using the GSEA algorithm of the piano package for R (Väremo *et al.*, 2013). Log2 fold changes were used as gene-level statistics, and *P*-values were estimated by gene sampling, followed by FDR adjustment for multiple hypothesis testing.

Gene Ontology (GO) terms related to identified proteins were visualized using REVIGO software (Supek *et al.*, 2011).

Results

Pigment accumulation

Chlorella vulgaris cells were acclimated to LL (70 µmol m^{-2} s^{-1}) or HL (850 µmol m^{-2} s^{-1}) growth conditions for at least 10 generations. We determined the light gradient experienced by the cell considering the pigment content and the transmittance of the culture on different days (Supplementary Fig. S1). The cells were exposed to a light gradient with the maximum range (bottom–top of the culture) of 70–30 µmol m^{-2} s^{-1} for LL cells and 850–390 µmol m^{-2} s^{-1} for HL cells. Cells grown in HL conditions were characterized by faster growth rate and increased biomass production compared with LL cells (Supplementary Fig. S2). As reported in Table 1, cells grown in HL were characterized

Published in : Journal of Experimental Botany (2023), vol. 74, n°15, pp. 4540-4558

DOI: 10.1093/jxb/erad170

Status : Postprint (Author's version)

by an ~60% reduction in Chl content per cell. Even stronger Chl reduction in HL cells was evident upon normalization to total protein content or to dry weight (Table 1). The residual Chl composition in HL samples was also changed compared with LL, with the Chl *a*/*b* ratio significantly increased at high irradiances. Carotenoid content was not significantly different on a cell basis but increased on a Chl basis in HL samples, with lutein representing ~70% of total carotenoids in both the LL and HL groups. In HL, zeaxanthin was also detectable, while the other xanthophylls (neoxanthin and violaxanthin) were significantly reduced on a cell basis in HL compared with LL. The reduced Chl *b* content and Chl/Car ratio in HL compared with LL suggest that exposure to different irradiances induced a reorganization of the photosynthetic apparatus.

Photosynthetic activity and mitochondrial respiration

The increased Chl *a*/*b* ratio in HL suggests a decrease of LHC antenna complexes per photosystem, since Chl *b* is only bound to external antenna subunits. Light-harvesting properties of PSII—also known as functional 'antenna size'—can be measured by following the Chl *a* fluorescence induction kinetics in DCMU-treated cells exposed to limiting light as fluorescence emission is inversely related to the light-harvesting properties of PSII. As shown in Fig. 1A, HL cells were characterized by slower fluorescence induction kinetics compared with LL cells, indicating a smaller PSII antenna size

Published in : Journal of Experimental Botany (2023), vol. 74, n°15, pp. 4540-4558

DOI: 10.1093/jxb/erad170

Status : Postprint (Author's version)

(Supplementary Table S1). In the case of PSI, its functional antenna size can be estimated by following the kinetics of P700 oxidation in limiting light in the presence of linear and cyclic electron transport inhibitors (DCMU and DBMIB) to fully inhibit P700 re-reduction, adding artificial electron donors and acceptors (ascorbate and methylviologen, respectively). As shown in Fig. 1B, there were no differences between HL and LL cells in the case of PSI antenna size.

LHCII antennae can migrate from PSII to PSI to balance the excitation pressure among the two photosystems in a process called state transitions (Finazzi *et al.*, 2002; Lemeille *et al.*, 2010; Nawrocki *et al.*, 2016). State transitions are triggered by the redox state of plastoquinones, with state 1 (S1) or state (S2) being the conditions with minimum or maximum migration of LHCII to PSI, respectively; they can be induced by consuming (S1) or increasing (S2) the reducing power in the chloroplast (Fleischmann *et al.*, 1999). When state transitions occur, the migration of LHCII to PSI increases its fluorescence emission, which consequently decreases the emission of PSII. S1 and S2 were then estimated by measuring fluorescence emission at 77K, where both PSI and PSII emissions are detectable. As shown in Fig. 1, increased state transition capacity was measured for LL-acclimated cells. This could be related to the presence of mobile LHC antenna proteins that might be lost upon HL acclimation.

Published in : Journal of Experimental Botany (2023), vol. 74, n°15, pp. 4540-4558

DOI: 10.1093/jxb/erad170

Status : Postprint (Author's version)

Table 1. *HPLC analysis of pigment content in C. vulgaris cells grown in LL or in HL conditions*

	Chl a/b	Chl/ Car	Neo/cell	Vio/ cell	Anthera/cell	Lut/ cell	Zea/cell	β car/ cell	Chl/ cell	Car tot/ cell	Chl/ prot	Car/ prot	Chl/DW	Car/DW
LL	3.24	2.59	0.23	0.22	ND	0.99	n.d.	0.24	4.36	1.92	105.71	40.81	33.62	12.98
SD	0.40	0.12	0.04	0.04	–	0.19	–	0.05	0.81	0.37	33.27	10.59	7.38	1.63
HL	4.19	1.01**	0.06**	0.16*	0.04**	1.02	0.25**	0.24	1.77**	1.81	40.98**	40.57	7.73**	7.65*
SD	0.84	0.01	0.01	0.02	0.02	0.04	0.02	0.02	0.06	0.06	7.10	1.23	1.44	1.43

Anthera, antheraxanthin; β car, β carotene; Chl, chlorophyll; Car, carotenoids; HL, high light; LL, low light; ND, not detectable; Neo, neoxanthin; Vio, violaxanthin; Zea, zeaxanthin; Car tot: total carotenoids. Chlorophyll and carotenoid contents per cell are reported as pmol per 1 × 10^7 cells. Chlorophyll and carotenoid content per total proteins (Chl/prot and Car/prot) or per dry weight (Chl/DW and Car/DW) are reported as pmol per mg of protein or mg of dry weight. Errors are reported as SD (n=4). *P<0.05 or **P<0.01 for HL versus LL.

Figure 1.

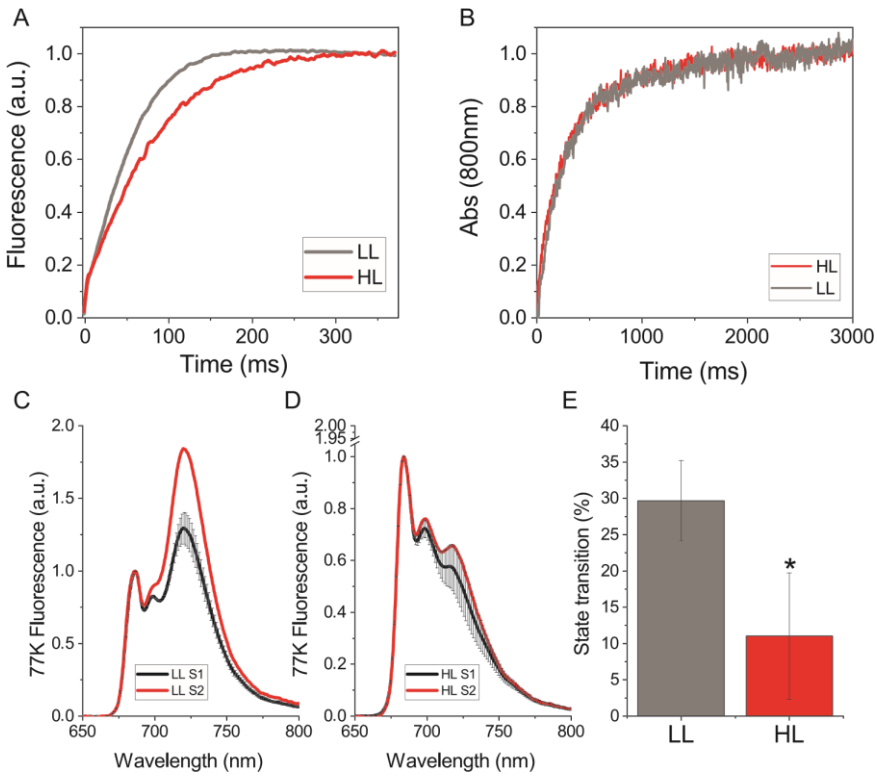

Published in : Journal of Experimental Botany (2023), vol. 74, n°15, pp. 4540-4558

DOI: 10.1093/jxb/erad170

Status : Postprint (Author's version)

Functional antenna sizes of PSI and PSII, and the state transitions. (A) Chl *a* fluorescence emission kinetics of whole cells grown in low light (LL) or high light (HL) treated with DCMU (representative of three independent biological replicates), related to the light-harvesting efficiency of PSII. (B) Kinetics of PSI reaction center oxidation followed by pump–probe differential absorption at 800 nm measured in whole cells treated with DCMU, methyl-viologen, and ascorbate (representative of three independent biological replicates) as described in the Materials and methods. (C and D) Chl *a* fluorescence emission spectra measured at 77K for cells grown in LL (C) or HL (D) in state 1 (S1) or state 2 (S2); S1 was induced in LL (~5 μmol m^2 s^{-1}) with 10 μM DCMU to oxidize the plastoquinone pool, while S2 was induced by adding 250 μM sodium azide to inhibit mitochondrial respiration and reduce the plastoquinone pool. (E) Extent of state transition retrieved from fluorescence emission spectra reported in (C) and (D) from the maximum fluorescence emission at 720 nm as (FS2–FS1)/FS2. Error bars are reported as SDs (n=3). * P<0.05 for HL versus LL.

Photosynthetic linear electron transport was then investigated by measuring light-dependent oxygen evolution. As shown in Fig. 2A, on a Chl basis, HL-acclimated cells were characterized by a higher oxygen evolution rate at light intensities >500 μmol m^{-2} s^{-1}, with an almost 3-fold increase in the maximum oxygen evolution rate (Pmax, Table 2). Due to reduced Chl per cell content, on a cell basis HL cells were evolving less oxygen compared with LL cells at lower actinic lights, but a similar oxygen production was achieved at a higher illumination range (Supplementary Fig. S3). HL-acclimated cells were thus more efficient on a Chl basis in using the available light energy to strip electrons from water molecules and transport them across the photosynthetic electron transport chain. The impact of cyclic electron transport compared with linear electron transport was then

Published in : Journal of Experimental Botany (2023), vol. 74, n°15, pp. 4540-4558

DOI: 10.1093/jxb/erad170

Status : Postprint (Author's version)

evaluated by measuring the ECS in the presence or absence of DCMU, which inhibits linear electron transport. ECS is directly related to thylakoid membrane polarization due to electron and proton transport; in the presence of DCMU, the ECS signal is only related to cyclic electron transport. In the absence of DCMU, there were no significant differences when comparing HL- with LL-acclimated cells (Fig. 2B). However, in the presence of DCMU, reduced ECS was evident in the case of LL-acclimated cells.

The relative contribution of cyclic electron transport to the ECS signal is reported in Fig. 2C for HL- and LL-acclimated cells at the different actinic lights measured, being significantly higher for HL cells. The increased cyclic electron transport contribution to overall photosynthetic electron transport suggests an increased ATP/NADPH ratio in HL for the cofactors produced in the light phase of photosynthesis, as cyclic electron transport is only related to lumen acidification and ATP biosynthesis.

PSI and PSII photosynthetic activities were then measured in HL- compared with LL-acclimated cells. In the case of PSI, P700 photochemical activity on a Chl basis was higher in HL versus LL (Fig. 3A). PSII photosynthetic properties were then analyzed by measuring the fluorescence-based parameters Y(II), 1–qL, and NPQ (Fig. 3B–E), representing the PSII quantum yield, the redox state of plastoquinone, and the capacity to thermally dissipate the light energy absorbed, respectively. Y(II) was higher for HL-acclimated cells for actinic

Published in : Journal of Experimental Botany (2023), vol. 74, n°15, pp. 4540-4558

DOI: 10.1093/jxb/erad170

Status : Postprint (Author's version)

lights up to 1400 µmol m^{-2} s^{-1}, indicating increased photochemical efficiency. Consistently, 1–qL values were lower in the same light range in HL cells, suggesting that the plastoquinone pool was less reduced and the photosynthetic electron transport chain less saturated.

Figure 2.

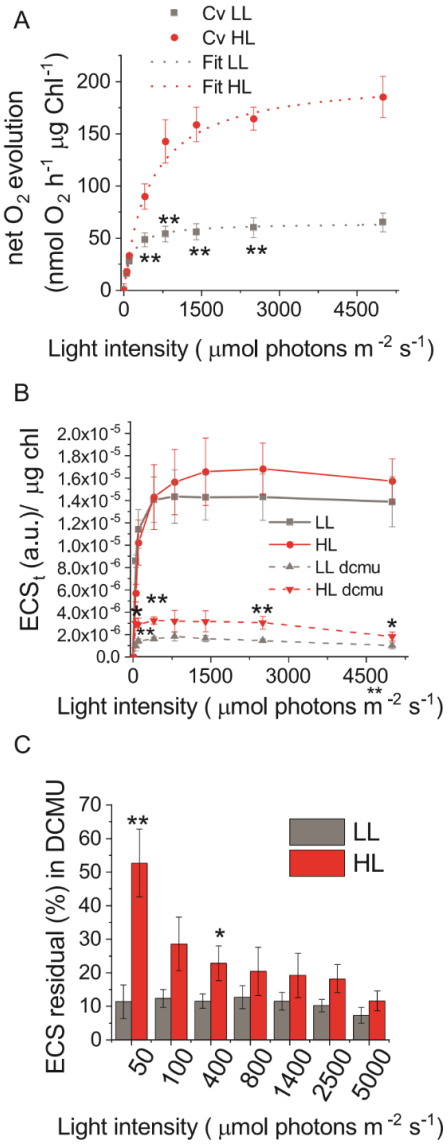

Published in : Journal of Experimental Botany (2023), vol. 74, n°15, pp. 4540-4558

DOI: 10.1093/jxb/erad170

Status : Postprint (Author's version)

Oxygen evolution and electrochromic shift (ECS) measurements. (A) Light curves of LL- and HL-acclimated cells measured as net lightdependent oxygen evolution rates at different actinic lights. Experimental data were fitted with hyperbolic functions, and fitting results are shown as dotted lines. (B) ECS measurements at different actinic lights for LL and HL cells in the presence (dotted lines) or absence (solid lines) of DCMU. (C) Percentage of residual ECS upon DCMU treatment compared with untreated cells; the residual ECS may be related to cyclic electron transport. Data are the means of three biological replicates with error bars showing the SDs. **P*<0.05 or ***P*<0.01 for HL versus LL.

Table 2. Oxygen evolution

	LL	HL
Pmax (μmol O_2 h^{-1} μg Chl^{-1})	64.68 ± 1.49	204.50 ± 5.92**
Half-saturation intensity (μmol photons m^{-2} s^{-1})	142.78 ± 6.50	509.39 ± 26.72**
Light compensation point (μmol photons m^{-2} s^{-1})	22.59 ± 4.33	123.50 ± 24.55**

The light curves in Fig. 2A were fitted by hyperbolic functions to determine the photosynthetic parameters Pmax and half-saturation intensity. Halfsaturation intensity, actinic light intensity at which the oxygen evolution rate is Pmax/2; HL, high light; LL, low light; Pmax, maximum light-dependent net oxygen evolution rate; Light compensation point, light intensity at which light-dependent oxygen evolution is equal to respiratory oxygen consumption. Dark respiration values normalized on a cell or chlorophyll basis are reported for LL- and HL-acclimated cells. ***P*<0.01 for HL versus LL.

The activity of PTOX in LL and HL cells was then investigated, being correlated to plastoquinone oxidation by chlororespiration. PTOX activity can be measured following the PSII fluorescence kinetics upon light to dark transition in the presence or absence of

Published in : Journal of Experimental Botany (2023), vol. 74, n°15, pp. 4540-4558

DOI: 10.1093/jxb/erad170

Status : Postprint (Author's version)

the PTOX inhibitor *n*-propylgallate (PG) (Houille-Vernes *et al.*, 2011). As shown in Supplementary Fig. S4, in the case of LL cells, light to dark transition caused a fast decay of fluorescence emission, which was delayed in the presence of PG. This result demonstrates that PTOX is active in LL cells and contributes to plastoquinone oxidation transferring electrons to oxygen. In the case of HL cells, a more complex situation was evident: without inhibitor, a transient dark rise of fluorescence was measured upon light to dark transition, suggesting that when the light is turned off a transient plastoquinone pool reduction occurs due to the high reducing power in the chloroplast which cannot be consumed by the carbon fixation pathway. In the presence of PG, HL cells were characterized by a continuous rise of fluorescence upon light to dark transition, indicating an important effect of PTOX on relaxing the plastoquinone pool which is essential in HL cells to properly balance the redox state of plastoquinones.

NPQ induction was characterized by complex kinetics: NPQ was induced to a higher level in HL-acclimated cells exposed to actinic light compared with the case for LL; however, after ~1 min of light exposure, NPQ relaxed and reached values similar to LL cells. When actinic light was turned off, NPQ dark relaxation was reduced in LL cells compared with HL, demonstrating increased qE induction in HL, as qE is the fast-relaxing component of NPQ induced by lumen acidification. This behavior was observed for all the different

Published in : Journal of Experimental Botany (2023), vol. 74, n°15, pp. 4540-4558

DOI: 10.1093/jxb/erad170

Status : Postprint (Author's version)

actinic lights (Supplementary Fig. S5). NPQ relaxation during actinic light exposure was suggested to be related to the activation of Calvin cycle enzymes that consume NADPH and ATP and restore their precursors $NADP^+$ and ADP, which are required to desaturate the photosynthetic electron transport chain (Cardol *et al.*, 2010).

NAD(P)H/NAD(P) balance was thus analyzed following fluorescence emission at ~500 nm, where the reduced NAD(P) H form is emitted. It is important to note that is not possible to discriminate between NADH and NADPH following 500 nm fluorescence emission, and the results obtained are related to the overall balance of NAD(P)H oxidation and reduction in the whole cell. As depicted in Fig. 3F, NAD(P)H fluorescence was initially increased upon exposure to actinic light in both LL and HL, indicating $NADP^+$ reduction; in the case of HL-acclimated cells, NADPH fluorescence emission reached a steady state, resulting from a similar rate of NADPH oxidation and $NADP^+$ reduction. In LL-acclimated cells, a continuous increase in NAD(P)H fluorescence was measured during actinic light exposure, suggesting relatively faster $NAD(P)^+$ reduction than NADPH oxidation, with a consequent decrease in the amount of $NAD(P)^+$ available as acceptors for electrons transported across the photosynthetic electron transport chain. These results are indeed consistent with the increased photosynthetic rates measured on a Chl basis in HL cells at the actinic light herein used for NAD(P)H measurement, and with the increased PTOX

Published in : Journal of Experimental Botany (2023), vol. 74, n°15, pp. 4540-4558

DOI: 10.1093/jxb/erad170

Status : Postprint (Author's version)

activity being able to prevent over-reduction of chloroplast reducing power (Fig. 2A). When the light was turned off, the NAD(P)H fluorescence signals decreased in both LL- and HL-acclimated cells, but the signal slowly and partially recovers after a few seconds, indicating ongoing $NAD(P)^+$ reduction that is likely to be related to light-independent NAD(P)H formation through the pentose phosphate pathway and/or by glycolysis and tricarboxylic acid (TCA) pathways.

Next, we evaluated mitochondrial respiration (Fig. 4) and found an increased oxygen consumption rate in the dark in the case of HL-acclimated cells compared with LL. Accordingly, the light compensation point measured for HL cells was higher compared with LL cells (Table 1). The contribution of cytochrome and alternative pathways was then investigated by measuring dark respiration in the presence of two specific inhibitors: SHAM that inhibits AOX and the alternative pathway, and myxothiazol that locks complex III, thereby blocking the cytochrome pathway (Dang *et al.*, 2014). The sums of the estimated alternative and cytochrome respiratory pathways, even if slightly lower, were not significantly different compared with the total dark respiration measured in the absence of inhibitors. The increased mitochondrial respiration in HL-acclimated cells was due specifically to the increased alternative pathway activity (Fig. 4). Electron transport through AOX is not coupled with proton transport across the inner mitochondrial

Published in : Journal of Experimental Botany (2023), vol. 74, n°15, pp. 4540-4558

DOI: 10.1093/jxb/erad170

Status : Postprint (Author's version)

membrane, and it does not support ATP biosynthesis. The relatively higher alternative pathway activity in HL-acclimated cells indicates more rapid regeneration of NAD^+. Higher AOX and PTOX activity in HL-acclimated cells probably allows correct tuning of the reducing power of chloroplasts and mitochondria, preventing over-reduction of electron transport carriers, consistent with the case of the extremely high light-tolerant strain *Chlorella ohadii* (Treves *et al.*, 2020; Kedem *et al.*, 2021).

Proteomic analysis

To investigate the molecular details underlying acclimation to HL or LL conditions, we performed a comparative proteomic analysis on protein extracts from acclimated cells. Microalgal proteins were extracted, digested, and purified to obtain peptides, which were separated using reversed-phase nanoLC and analyzed by an Orbitrap mass spectrometer (see the Materials and methods for details). A direct data-independent acquisition (directDIA) method was leveraged to determine protein compositions and differential protein abundances under the two acclimation conditions. In total, 4457 proteins were identified and quantified (Supplementary Dataset S1), demonstrating an improved resolution compared with previous proteomic datasets obtained from *C. vulgaris*, where <3000 proteins were identified (Guarnieri *et al.*, 2013). Protein content per cell was similar in HL and LL cells (Supplementary Fig. S6A), but the protein

Published in : Journal of Experimental Botany (2023), vol. 74, n°15, pp. 4540-4558

DOI: 10.1093/jxb/erad170

Status : Postprint (Author's version)

percentage of dry weight was reduced in HL (Supplementary Fig. S6B), consistent with previous finding (Cecchin *et al.*, 2019). Differential protein expression was then analyzed (Fig. 5). It is important to note that even if the different replicates analyzed were characterized by a similar growth curve for each condition (Supplementary Fig. S2), there was more variance in HL cells compared with LL cells in terms of protein expression as reported by principal component analysis (PCA) (Fig. 5A), suggesting a more dynamic adjustment of protein expression in the former: the higher growth rates of HL cells compared with LL cells imply a faster transition between the different cell growth phases, possibly increasing the variance during samplings. The volcano plot obtained upon expression analysis demonstrates that most of the identified proteins were not differentially expressed in HL versus LL conditions (Fig. 5B). Accordingly, considering adjusted *P*-values below 0.05, only 89 and 147 proteins were up-regulated and down-regulated, respectively, in HL, with a log2 fold change >1 or < –1 (Supplementary Dataset S2). The top 10 up-regulated or down-regulated proteins in HL versus LL are shown in Fig. 5C. GSEA was then performed on the GO terms retrieved (Fig. 5D); significant results were obtained only for GO terms down-regulated in HL, most of which were involved in the light phase of photosynthesis as PSI and PSII components, Chl-binding proteins, and/or proteins located in the thylakoidal membranes. This result is consistent with the decrease in Chl content per cell observed in HL versus LL cells (Table 1). Moreover,

Published in : Journal of Experimental Botany (2023), vol. 74, n°15, pp. 4540-4558

DOI: 10.1093/jxb/erad170

Status : Postprint (Author's version)

significant enrichment of proteins with peptidyl-prolyl isomerase activity was iden- chains, a key step for protein folding. Significant enrichment tified as down-regulated in HL (Supplementary Table S2): of GO terms encoding cytosolic large ribosomal subunits was peptidyl-prolyl isomerases catalyze *cis–trans* isomerization of also identified as down-regulated in HL, suggesting a general peptide bonds N-terminal to proline residues in polypeptide decrease of protein biosynthesis in HL cells, consistent with the reduced percentage of protein content per dry weight at high irradiance. To provide a more general view of the protein expression in HL versus LL conditions, GO terms resulting after GSEA with an adjusted *P*-value <0.25 were visualized by the REVIGO tool (Supek *et al.*, 2011) analyzing separately the enriched GO terms which were up-regulated or downregulated in HL (Supplementary Fig. S7). In addition to the main GO terms down-regulated in HL, such as those involved in photosynthesis and peptidyl-prolyl isomerases, REVIGO analysis allowed the identification of 'ATP binding' and 'intracellular transport' as enriched GO terms up-regulated in HL at the limit of significance (adjusted *P*-value of 0.056). Moreover, the most significant enriched GO terms referring to cellular compartments were related to the mitochondria for up-regulated genes and to the chloroplast envelope, plastoglobuli, and photosystems for genes down-regulated in HL versus LL. The GO terms and KEGG orthology identifiers of the differentially expressed

Published in : Journal of Experimental Botany (2023), vol. 74, n°15, pp. 4540-4558

DOI: 10.1093/jxb/erad170

Status : Postprint (Author's version)

proteins were then used to analyze their functions are described below and summarized in Fig. 6.

Figure 3.

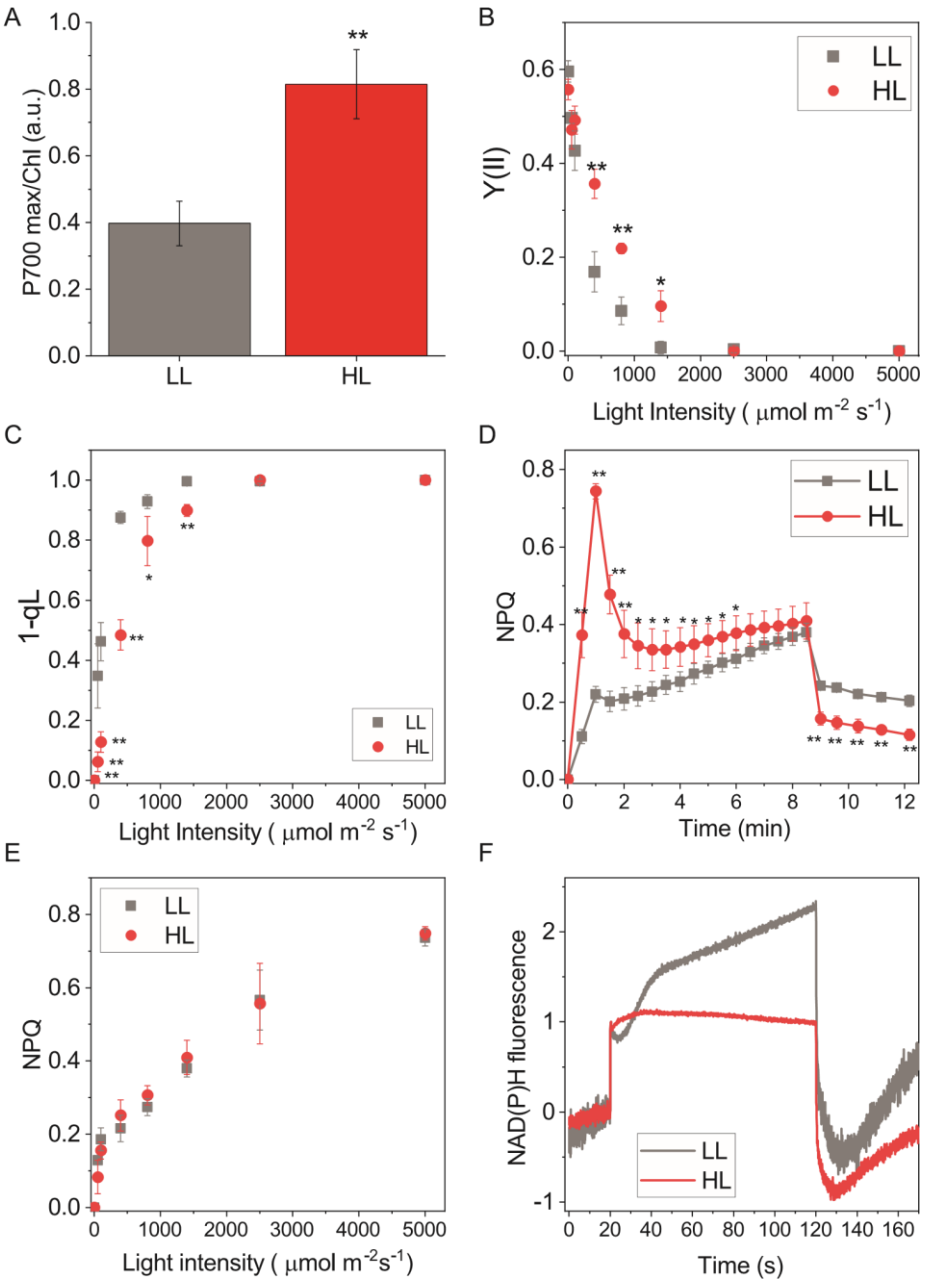

Photosynthetic parameters and NAD(P)H reduction rates. (A) Maximal PSI activity (P700 oxidation) on a chlorophyll basis measured in LL- or HL-acclimated cells. (B and C) PSII quantum yield (B) and 1–qL (reduced

Published in : Journal of Experimental Botany (2023), vol. 74, n°15, pp. 4540-4558

DOI: 10.1093/jxb/erad170

Status : Postprint (Author's version)

Q_A fraction, C), at different actinic light intensities for LL- or HL-acclimated cells. (D) NPQ kinetics measured upon exposure of dark-adapted LL or HL cells to 1400 µmol m^{-2} s^{-1} actinic light for 8 min followed by dark relaxation. (E) NPQ values at the end of the actinic light exposure as described in (D) at different actinic light intensities for LL- or HL-acclimated cells (see Supplementary Fig. S1 for more details). Data are means of three biological replicates with error bars showing the SDs. (F) Kinetics of NAD(P) H fluorescence emission measured on dark-adapted LL or HL cells: actinic light (1400 µmol m^{-2} s^{-1}) was turned on after 20 s and turned off at 120 s. NAD(P)H fluorescence emission kinetics were normalized to the initial rise upon exposure to actinic light. **P*<0.05 or ***P*< 0.01 for HL versus LL.

Figure 4.

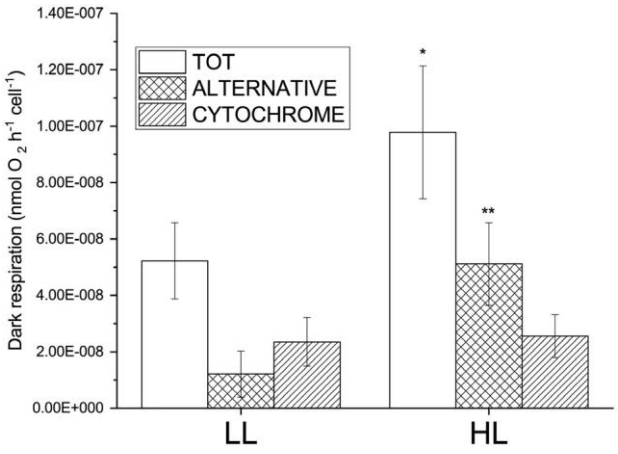

Dark respiration of *Chlorella vulgaris* cells grown in LL or HL conditions. Dark respiration is reported as total dark respiration measured in the absence of inhibitors (TOT) and the relative contribution of cytochrome (CYTOCHROME) and alternative respiration (ALTERNATIVE) measured in the presence of SHAM or mixothiazol, inhibiting AOX and complex III, respectively. Data are the means of three biological replicates with error bars showing the SDs. **P*<0.05 or ***P*<0.01 for HL versus LL.

Published in : Journal of Experimental Botany (2023), vol. 74, n°15, pp. 4540-4558

DOI: 10.1093/jxb/erad170

Status : Postprint (Author's version)

Photosynthesis

Cells acclimated to HL were characterized by down-regulation of several proteins annotated as LHC subunits. In particular, most of the proteins previously annotated in *C. vulgaris* as antenna proteins of PSI (Lhca) or PSII (Lhcb) (Cecchin *et al.*, 2019) were down-regulated in HL-acclimated cells. Similarly, several subunits of the PSI and PSII core complexes were down-regulated in HL (Supplementary Table S3). These results are consistent with the reduced Chl content per cell measured in HL compared with LL (Table 1). The reduced accumulation of PSI, PSII, and LHCII subunits was then confirmed by western blot analysis using α-PsaA (subunit of PSI core complex), α-CP43 (subunit of PSII core complex), and α-LHCII antibodies (Supplementary Fig. S8). HL cells also showed down-regulation of Low PSII Accumulation (LPA) protein expression. These proteins are involved in PSII assembly, and gene deletions in *Arabidopsis thaliana* or *C. reinhardtii* severely impaired PSII accumulation (Schneider *et al.*, 2014; Cecchin *et al.*, 2021a; Wakao *et al.*, 2021; Spaniol *et al.*, 2022). Interestingly, no significant differential expression for proteins involved in carbon fixation was found in HL versus LL *C. vulgaris* cells (Supplementary Dataset S3). This result was confirmed on a cell basis by western blot analysis in the case of the large subunit of Rubisco (Supplementary Fig. S8). It is interesting to note that, as the Chl content per cell is reduced in HL, the similar Rubisco

Published in : Journal of Experimental Botany (2023), vol. 74, n°15, pp. 4540-4558

DOI: 10.1093/jxb/erad170

Status : Postprint (Author's version)

content per cell means an increased accumulation of the main enzyme involved in carbon fixation on a Chl basis in HL conditions; the increased Rubisco content per Chl could contribute to the increased electron transport properties measured in the case of HL cells, due to increased regeneration of ATP and NADPH precursors. A protein predicted as chloroplast ferredoxin-thioredoxin reductase (g1978.t1) was down-regulated in HL. This enzyme is involved in activation of Calvin cycle enzyme depending on the redox state of the chloroplast. The plastid localization of the g1978.t1 gene product was confirmed by TargetP, and its down-regulation in HL indicates that thioredoxin-based activation of the Calvin cycle enzyme is required more in LL rather than in HL conditions. Finally, HL cells were characterized by reduced accumulation of proteins encoded by g10107. t1 and g5581.t1 genes, predicted as carbonic anhydrase, a component of the CCM (carbon-concentrating mechanism). The CCM is found in microalgae and enables an increased intracellular concentration of CO_2 (Wang *et al.*, 2015; Yamano *et al.*, 2008). It is possible that the increased carbon flow and mitochondrial respiration in HL conditions enhance CO_2 concentrations in the cells, which would induce a decrease in CCM activity (Fig. 6).

Pigment biosynthesis

Coproporphyrinogen III oxidase (g5001.t1), chlorophyll(ide) *b* reductase (g9809.t1), and porphobilinogen deaminase (g4163. t1) are enzymes involved in Chl biosynthesis and

Published in : Journal of Experimental Botany (2023), vol. 74, n°15, pp. 4540-4558

DOI: 10.1093/jxb/erad170

Status : Postprint (Author's version)

were reduced in HL-acclimated cells. This observation is consistent with the reduced Chl content per cell observed for HL compared with LL. In the case of carotenoid biosynthesis, the only enzyme identified as significantly differentially expressed was zeaxanthin epoxidase (g9297.t1), which was down-regulated in HL, while the violaxanthin de-epoxidase enzyme was down-regulated in HL at the limit of the threshold herein considered (*P*-value of 0.05 and log2 fold change >1; Supplementary Dataset S3). Both zeaxanthin epoxidase (ZE) and violaxanthin de-epoxidase (VDE) are involved in zeaxanthin metabolism: ZE catalyzes the epoxidation of zeaxanthin to antheraxanthin and violaxanthin, while VDE is the enzyme that upon light stress triggers the conversion of violaxanthin into zeaxanthin.

The decreased expression of ZE in HL cells is in line with the increased zeaxanthin fraction of total carotenoids measured in HL-acclimated cells (Table 1). Similarly, the reduced violaxanthin content in HL reduces the requirement for the VDE enzyme as a significant fraction of zeaxanthin has already accumulated. It is important to note that zeaxanthin is involved in several photoprotective mechanisms in *C. vulgaris* (Girolomoni *et al.*, 2020).

Published in : Journal of Experimental Botany (2023), vol. 74, n°15, pp. 4540-4558

DOI: 10.1093/jxb/erad170

Status : Postprint (Author's version)

Figure 5.

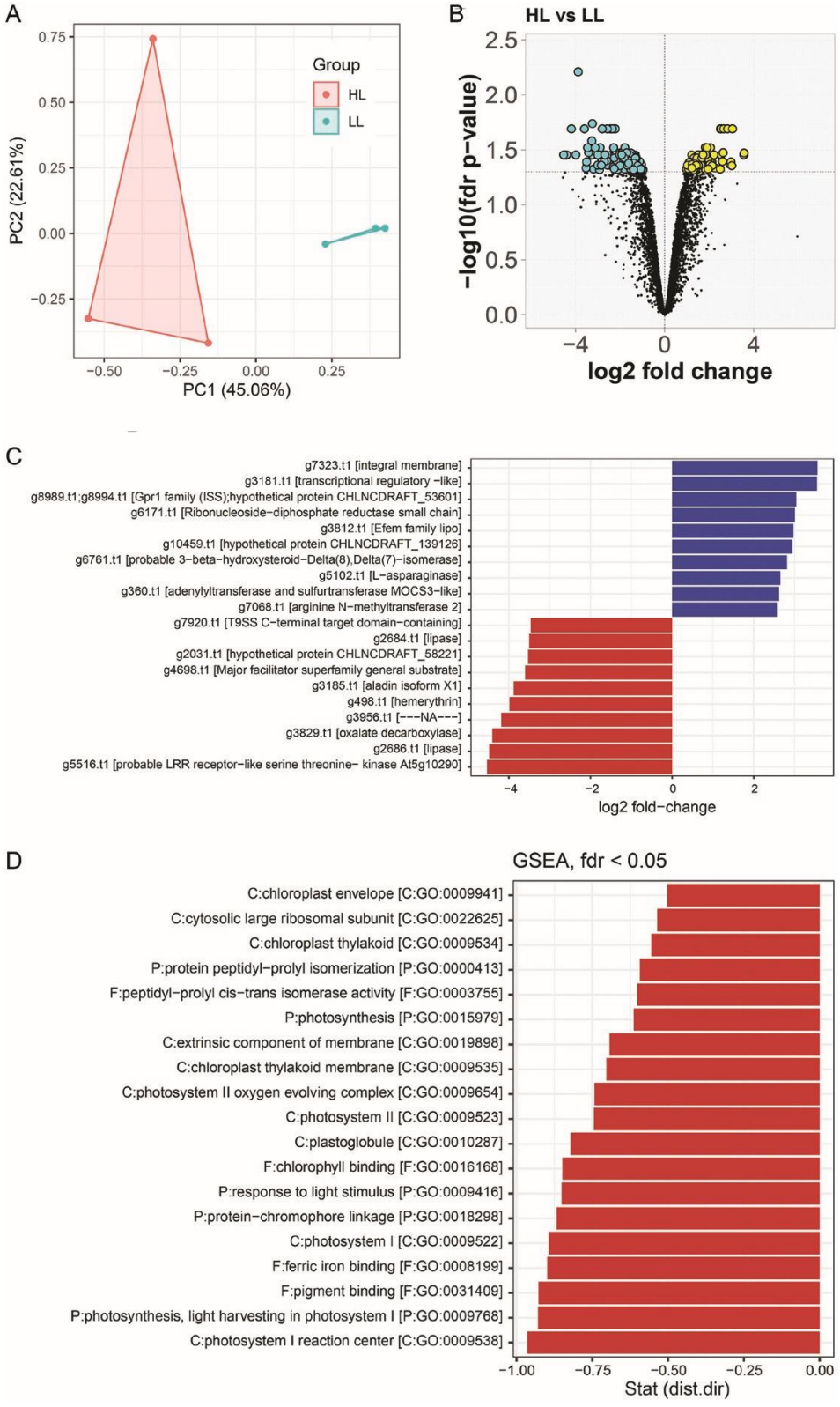

Published in : Journal of Experimental Botany (2023), vol. 74, n°15, pp. 4540-4558

DOI: 10.1093/jxb/erad170

Status : Postprint (Author's version)

Analysis of differentially expressed proteins in HL- versus LL-acclimated *Chlorella vulgaris* cells. (A) PCA of the replicates analyzed for HL and LL samples. (B) Volcano plots representing the systems response profiles. For each protein, the protein expression change (calculated as the log2 fold change) is plotted on the *x*-axis and the statistical significance (proportional to the negative log10-adjusted *P*-value) is plotted on the *y*-axis. Yellow and cyan dots highlight proteins that are statistically significantly up- and down-regulated, respectively (FDR-adjusted $P<0.05$). (C) Top 10 proteins up- or down-regulated in HL versus LL by log2 fold change. (D) GSEA performed on GO terms. Gene set statistics shown for significantly affected gene sets (FDR-adjusted *P*-value <0.05). Note that only down-regulated gene sets were identified as significantly enriched in the GSEA.

Figure 6.

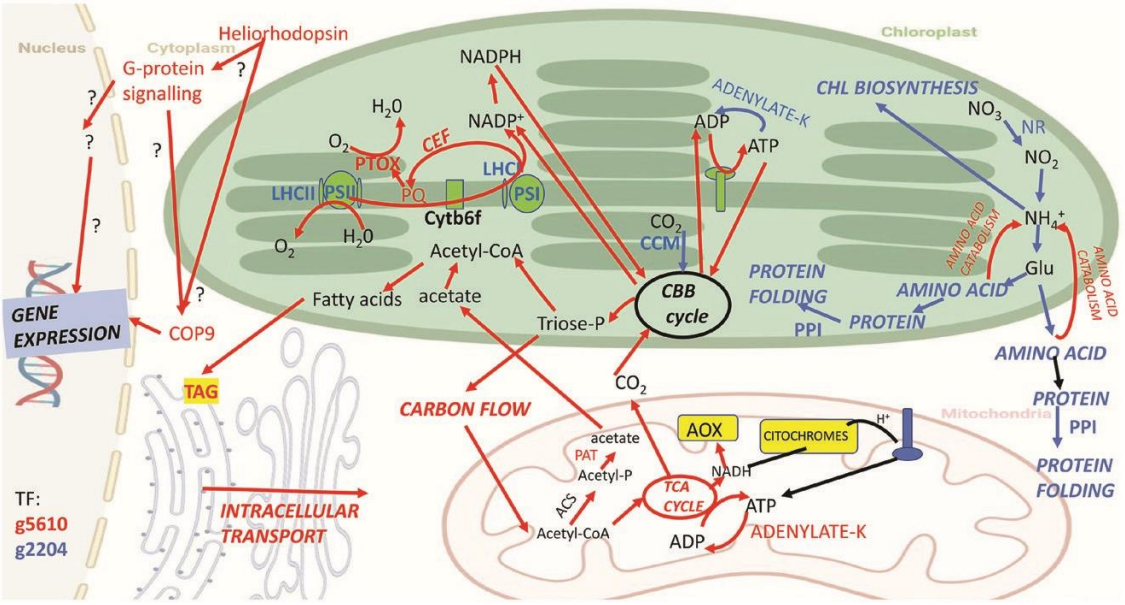

Schematic model of cell metabolism adaptation to LL or HL conditions. The model represented is based on the physiological measurements of photosynthetic activity and mitochondrial respiration, and of proteomic analysis described in this work. Red, blue, and black colors indicate metabolic flows or metabolite/protein concentrations estimated as up-regulated, down-regulated, or unchanged, respectively, in HL versus LL cells. The metabolic pathways are indicated in italics. The metabolic flux estimated as up-regulated, down-

Published in : Journal of Experimental Botany (2023), vol. 74, n°15, pp. 4540-4558

DOI: 10.1093/jxb/erad170

Status : Postprint (Author's version)

regulated, or unchanged derives from a model based on enzyme concentration (proteins determined as differentially expressed by proteomic analysis are reported in red or blue for up- or down-regulated proteins). Only in the case of photosynthetic electron flow, cyclic electron flow (CEF), and mitochondrial respiration are the estimated fluxes derived from experimental data. The background of the figure representing the intracellular structure was obtained with BioRender software. PPI, peptidyl-proyl isomerase; NR, nitrate reductase; AOX, alternative oxidase; LHCI/II, light-harvesting complex I/II; TF, transcription factor; ACS, acetyl-CoA synthase; PAT, phosphate acetyltransferase; Chl, chlorophyll; CCM, carbon-concentrating mechanism; PTOX, Plastid Terminal Oxidase; CBB, Calvin–Benson-Basham cycle; Adenyklate-K, adenylate kinase; Cytb6f, cytochrome b_6f.

Nitrogen assimilation and amino acid metabolism

Ferredoxin nitrate reductase (g9255.t1) was down-regulated in HL-acclimated cells. Nitrate reductases are chloroplast enzymes required for nitrogen assimilation to produce ammonia from nitrate, which was provided to LL and HL cells as the nitrogen source during growth. Considering the requirement of ammonia for Chl biosynthesis, nitrate reductase expression is likely to be linked with the regulation of the accumulation of pigments at different growth irradiances. Accordingly, ferredoxin nitrate reductase expression was reduced in HL conditions, as was the Chl content per cell. Considering the increased growth rate observed for cells grown in HL, we cannot exclude that nitrogen assimilation fluxes could be similar or even increased in HL versus LL cells due to post-translational regulation. Nitrate assimilation was also reported in *A. thaliana* (Lea *et al.*, 2006) and *C. reinhardtii* (González-Ballester *et al.*, 2004) as being regulated by the

Published in : Journal of Experimental Botany (2023), vol. 74, n°15, pp. 4540-4558

DOI: 10.1093/jxb/erad170

Status : Postprint (Author's version)

intracellular concentration of amino acids, even if this mechanisms has not been fully elucidated yet in the case of green algae (Sanz-Luque *et al.*, 2015).

Several enzymes involved in amino acid catabolic metabolism were up-regulated in HL-acclimated cells, including 2-oxoisovalerate dehydrogenase E1 component alpha subunit (g10682.t1) and 3-methylcrotonyl-CoA carboxylase alpha subunit (g10016.t1) involved in leucine degradation, with the former also catalyzing reactions involved in valine and isoleucine degradation. In HL-acclimated cells, enzymes catalyzing transfer or removal of nitrogenous groups were also up-regulated, such as l-asparaginase (g5102.t1) and aromatic amino acid aminotransferase II (g7030.t1). Moreover, increased accumulation of three proteases was observed in HL (g8295.t1, g1394.t1, and g10206.t1); up-regulation of enzymes involved in amino acid degradation could be related to a strategy to recycle the amino group when nitrate reductase expression is decreased. Increased amino group recycling could also be related to increased photooxidative stress in HL cells and increased protein damage.

Intracellular transport and trafficking

Several proteins involved in intracellular transport and trafficking were up-regulated in HL (Supplementary Table S4), including a Sec24-like subunit involved in vesicle formation.

Published in : Journal of Experimental Botany (2023), vol. 74, n°15, pp. 4540-4558

DOI: 10.1093/jxb/erad170

Status : Postprint (Author's version)

Moreover, several intracellular and extracellular transport components were up-regulated in HL, including transporters for amino acids (g8327.t1, g1827.t1, g1828.t1, and g9008.t1). In contast, HL cells showed down-regulation of a peptide ABC transporter (g6888.t1). These findings suggest a reorganization of amino acid and peptide transport in cells upon acclimation to different light intensities. These results could be linked to the increased expression of amino acid catabolic enzymes and reduced protein content per dry weight in HL cells. It is interesting to note that in HL cells a protein annotated as being in the MATE (multidrug and toxic compound extrusion) efflux family (g9504.t1) was strongly up-regulated. The MATE protein family was reported to be involved in detoxification processes in different organisms, including land plants and microalgae (Nimmy *et al.*, 2022). The increased accumulation of a MATE protein in HL cells suggests a role for this subunit in HL acclimation.

Sulfur assimilation

Sulfur assimilation requires sulfate import into cells, which is activated by adenylation of adenosine 5'-phosphosulfate (APS). APS can then be reduced to produce sulfite, which can be used for cysteine and methionine biosynthesis, or phosphorylated to produce PAPS (3'-phosphoadenosine-5'-phosphosulfate), which serves as a sulfate donor to synthesize sulfated metabolites (Klein and Papenbrock, 2004). In the case of the sulfur

Published in : Journal of Experimental Botany (2023), vol. 74, n°15, pp. 4540-4558

DOI: 10.1093/jxb/erad170

Status : Postprint (Author's version)

assimilation pathway, the enzyme adenylyl-sulfate kinase (g1541. t1) that catalyzes APS phosphorylation was down-regulated in HL. Down-regulation of enzymes involved in APS phosphorylation was previously observed in *A. thaliana* in the setting of sulfur deficiency, when sulfate transporters are up-regulated (Bohrer *et al.*, 2014). Consistently, a sulfate transporter (g7389. t1) was up-regulated in HL-acclimated cells, while a predicted homocysteine *S*-methyltransferase (g5360.t1) involved in methionine biosynthesis was down-regulated in HL. Moreover, up-regulation of adenylyl-transferase and sulfotransferase MOCS3-like protein (g360.t1) was observed in HL cells; this enzyme is involved in molybdenum cofactor biosynthesis and thiocarboxylation of the adenylated C-terminal glycine of the ubiquitin-related modifier 1 (URM1) (Mayr *et al.*, 2021). URM1 is involved in either thiolation of tRNA or urmylation of target proteins (Schmitz *et al.*, 2008; Nakai *et al.*, 2012). Urmylation is a post-translation protein modification that is reportedly involved in oxidative stress in plants, and in nutrient sensing and budding in yeast (Goehring *et al.*, 2003). The role of urmylation in microalgae has not been sufficiently investigated, but in *C. vulgaris* a homolog of URM1 is encoded by gene g314.t1 (Supplementary Fig. S10), which was not differentially expressed in HL versus LL conditions.

Published in : Journal of Experimental Botany (2023), vol. 74, n°15, pp. 4540-4558

DOI: 10.1093/jxb/erad170

Status : Postprint (Author's version)

Nucleotide metabolism

HL-acclimated cells were characterized by up-regulation of a predicted ribonucleoside-diphosphate reductase (g6171. t1). This key enzyme for purine and pyrimidine metabolism catalyzes the formation of deoxyribonucleotides from ribonucleotides. Increased deoxynucleotide biosynthesis could be related to the higher growth rate observed in HL-acclimated cells (Cecchin *et al.*, 2019), as more DNA replication is required for cell division.

Lipid metabolism

Enzymes involved in lipid biosynthesis or catabolism were generally not differentially expressed in HL- versus LL-acclimated cells, with the exception of down-regulation of a caleosin/ peroxygenase 2-like protein (g8244.t1) in HL (Supplementary Dataset S3). This protein is a predicted calcium-binding peroxygenase involved in the degradation of oil bodies (Rahman *et al.*, 2018), and its down-regulation in HL is consistent with the increased lipid and triacylglycerol accumulation in HL cells previously reported for *C. vulgaris* (Cecchin *et al.*, 2019). A solanesyl diphosphate synthase (g5152.t1) was also up-regulated in HL. Solanesyl diphosphate synthase is an enzyme involved in ubiquinone and plastoquinone biosynthesis, where plastoquinones are required to desaturate the photosynthetic electron transport chain. Previous work demonstrated dual localization

Published in : Journal of Experimental Botany (2023), vol. 74, n°15, pp. 4540-4558

DOI: 10.1093/jxb/erad170

Status : Postprint (Author's version)

of solanesyl diphosphate synthase in the chloroplasts and mitochondria of plants (Ohara *et al.*, 2010). In the case of the g5152.t1 gene product, it was not possible to identify a transit peptide for chloroplasts or mitochondria, and further work is required to investigate the localization of function for this enzyme. Finally, enzymes involved in sterol biosynthesis were up-regulated in HL, including an NADPH:adrenodoxin reductase (g1319.t1), a cytochrome P450 (g7370.t1), and a 3-beta-hydroxysteroid-Δ8,Δ7-isomerase (g6761.t1). Steroid metabolites (ergosterol and brassicasterol) were previously shown to be produced in *Chlorella* species, and sterol content was reportedly enhanced at increasing irradiances in various microalgal species (Randhir *et al.*, 2020).

Mitochondrial oxidation pathways

A mitochondrial succinate dehydrogenase assembly factor (g8306.t1) was up-regulated in HL cells. Succinate dehydrogenase is an enzyme involved in the TCA cycle that strips electrons from succinate and reduces ubiquinone to fuel oxidative phosphorylation reactions. Increased accumulation of mitochondrial succinate dehydrogenase assembly factor is thus consistent with the higher level of mitochondrial respiration observed in HL. It is important to note that one of the proteins with the strongest up-regulation in HL-acclimated cells was a phosphate acetyltransferase (PAT encoded by g6335. t1). This enzyme catalyzes the reversible production of acetate from acetyl phosphate, which can

Published in : Journal of Experimental Botany (2023), vol. 74, n°15, pp. 4540-4558

DOI: 10.1093/jxb/erad170

Status : Postprint (Author's version)

be produced by acetyl-CoA synthase (ACS). The gene product of g6335.t1 has a predicted mitochondrial target peptide; in *C. reinhardtii*, ACS and PAT enzymes were identified in both the mitochondria and plastids, where they are involved in dark fermentation of sugars to produce acetate (Yang *et al.*, 2014). It is possible that the increased carbon flow in HL-acclimated cells enhances the production of acetyl-CoA, which can be converted into acetate that then diffuses back to the chloroplast or the cytosol as a precursor for fatty acid biosynthesis (Lin and Oliver, 2008; Cecchin *et al.*, 2019). Interestingly, HL-acclimated cells exhibited increased accumulation of a protein annotated as adenylate kinase (g3460.t1). Its localization is predicted in the mitochondria, while another two adenylate kinases located in chloroplasts (g1121.t1, g2609.t1) were down-regulated in the same growth conditions. Adenylate kinase enzymes are involved in the regulation of ATP, ADP, and AMP homeostasis; they catalyze the reversible reaction where a phosphate group is transferred from ATP to AMP to form two ADP molecules (Lange *et al.*, 2008). The reduced accumulation of adenylate kinase in chloroplasts in HL-acclimated cells can be explained by the increased requirement of ATP for CO_2 assimilation at high irradiances and the consequent continuous regeneration of ADP. Alternatively, considering the requirement of AMP for amino acid activation, reduced expression of AMP-producing adenylate kinase in the chloroplast could be associated with the reduced protein synthesis of photosynthetic subunits measured in HL versus LL cells. In contrast, the

Published in : Journal of Experimental Botany (2023), vol. 74, n°15, pp. 4540-4558

DOI: 10.1093/jxb/erad170

Status : Postprint (Author's version)

greater accumulation of mitochondrial adenylate kinase in HL cells could be related to increased carbon flow and mitochondrial respiration which require higher ADP availability for ATP production and relaxation of the proton gradient across the inner mitochondrial membrane generated by NADH oxidation. In the case of mitochondrial localization, adenylate kinase was suggested to only be present in the intermembrane space in plants (Stitt *et al.*, 1982), while in human cells adenylate kinase isoforms were found also in the mitochondrial matrix. No specific information is available for adenylate kinase localization in the case of green algae: considering its possible localization in the intermembrane space in *C. vulgaris*, a different possible role for mitochondrial adenylate kinase in HL acclimation is that this enzyme regulates the level of adenylates after export of ATP across the inner membrane by the ATP/ADP translocator, as previously suggested in the case of plants (Stitt *et al.*, 1982; Roberts *et al.*, 1997).

Signaling and gene expression

It is interesting to note that the protein with the highest fold change in HL compared with LL (g7323.t1, Fig. 5D) was found to have 71% and 80.7% identity and similarity, respectively, with a heliorhodopsin previously identified in *Chlorella variabilis* (Pushkarev *et al.*, 2018) (Supplementary Fig. S9). Heliorhodopsins are microbial-like rhodopsins previously suggested to have light-sensing activity (Kovalev *et al.*, 2020; Chazan *et al.*,

Published in : Journal of Experimental Botany (2023), vol. 74, n°15, pp. 4540-4558

DOI: 10.1093/jxb/erad170

Status : Postprint (Author's version)

2022), which could be required for adaptation of *C. vulgaris* cells to grow under high irradiance. In HL, other signaling proteins were identified among the top 10 up-regulated proteins, such as the Gpr1-like protein (g8989. t1; g8994.t1). Gpr1 is a member of the G protein-coupled receptor family and is likely to be a component of the signaling pathway underlying the physiological response triggered by HL acclimation. Notably, a protein annotated as TBC1 domain family member 2A (g4132.t1) was also up-regulated in HL. Proteins with TBC domains have been reported in different organisms from humans to plants as GTP-ase activating subunits that deactivate the signaling function of G proteins (Pan *et al.*, 2006), probably acting as a specific component of signaling pathways for cell acclimation in HL. Moreover, a subunit (subunit 6) of the COP9 signalosome (g8205.t1) was up-regulated in HL-acclimated cells. COP9 is a protein complex initially characterized in plants but then found in several eukaryotic organisms; it is involved in the activation of E3-cullin RING ubiquitin ligases (CRLs) that further control protein degradation through ubiquitination (Barth *et al.*, 2016). In plants, COP9 is a component of photoreceptor-mediated signaling (Wei *et al.*, 1994; Chamovitz *et al.*, 1996), and its increased accumulation in HL suggests a specific role in cell responses at higher irradiances, even if the role of COP9 in microalgae has not been fully elucidated. Several kinases and phosphatases were up-regulated in HL, while only a histidine kinase (g6989.t1) and an LRR (leucinerich repeat) receptor-like serine/threonine kinase (g5516.

Published in : Journal of Experimental Botany (2023), vol. 74, n°15, pp. 4540-4558

DOI: 10.1093/jxb/erad170

Status : Postprint (Author's version)

t1) were reduced in HL compared with LL-acclimated cells (Supplementary Table S5). LRR receptor-like serine threonine kinases belong to a multigene family considered to be the largest family of plant receptor kinases that is reportedly involved in plant development and immunity (Afzal *et al.*, 2008; De Smet *et al.*, 2009), but their relevance in microalgae remains unclear. Interestingly, three different gene products annotated as chloroplast aarF domain-containing kinase (g5742.t1, g9784.t1, and g7165.t1) were up-regulated in HL cells. The protein homolog of aarF domain-containing kinase in *A. thaliana* was renamed ABC1K1 (activity of bc1 complex kinase 1) and was associated with plastoglobuli with a role in triggering the biosynthesis of plastoquinone and carotenoid that are required to prevent or mitigate photo-oxidative stress (Martinis *et al.*, 2014). For this reason, ABC1K1 activity can be linked with HL acclimation mechanisms in *C. vulgaris* cells, which are more likely to experience photo-oxidative stress than cells grown in LL.

Transcription factors are usually in low abundance compared with other proteins, and their identification by proteomic analysis is not trivial (Simicevic and Deplancke, 2017; Simicevic *et al.*, 2013): here 83 different putative transcription factors were identified (Supplementary Dataset S3). Only two putative transcription factors were differentially expressed in HL versus LL cells. The products of genes g5610.t1 and g2204.t1 were both annotated as transcription factors and up-regulated and down-regulated in HL,

Published in : Journal of Experimental Botany (2023), vol. 74, n°15, pp. 4540-4558

DOI: 10.1093/jxb/erad170

Status : Postprint (Author's version)

respectively. Possibly, the differential expression of other transcription factors may have not been detected in our proteomic analysis due to the low abundance of these proteins. It is interesting to note HL up-regulation of proteins predicted to be HASTY1 (g1408.t1) and TRANSPORTIN1 (g10026. t1). Their homologous proteins in *A. thaliana* were reported to have a function in miRNA activity; HASTY1 favors the nuclear export of miRNA, while TRANSPORTIN1 mediates the interaction between miRNA and ARGONAUTE, a protein required for miRNA-mediated post-transcriptional regulation.

Discussion

Acclimation to different growth conditions is a key parameter to be considered for microalgae cultivation in artificial systems. Different cultivation set-ups imply varied exposure of cells to light, CO_2, nutrients, and temperature, which may significantly influence the biomass and biomolecular properties of the cultivated strains. In the case of *C. vulgaris*, our results reveal a different situation compared with the model organism for green algae *C. reinhardtii.* Indeed, *C. reinhardtii* acclimation to HL does not influence the stoichiometry of antenna subunits per PSII, but it is accompanied by a strong increase in its photoprotective properties, with increased capability for NPQ induction (Bonente *et al.*, 2012). In *C. vulgaris*, HL acclimation was associated with reduced

Published in : Journal of Experimental Botany (2023), vol. 74, n°15, pp. 4540-4558

DOI: 10.1093/jxb/erad170

Status : Postprint (Author's version)

accumulation of both LHC and the core subunits of PSI and PSII, with a reduced functional antenna size in the case of PSII, similar to the case of land plants acclimated to high irradiances (Ballottari *et al.*, 2007). *Chlorella vulgaris* HL-acclimated cells were also characterized by different NPQ dynamics compared with LL cells. Even if the total NPQ observed at the end of light exposure was similar in HL- and LL-acclimated cells, the former induced a higher qE (the fastest component of NPQ), and cells showed higher NPQ values during the first minute of illumination. The key proteins involved in qE, such as LHCSR (light-harvesting complex stress related) and PSBS subunits, were not differentially accumulated in HL versus LL cells; however, considering the reduced PSII core observed in HL, higher PSBS/PSII and LHCSR/ PSII contents are consistent with the observations of different NPQ dynamics and increased qE.

It is worth noting that when the cell concentration increased, in both LL and HL conditions, a light gradient was established across the cell cultures, as reported in Supplementary Fig. S1. The *C. vulgaris* cells were adapting to LL or HL conditions while also facing the challenge of light fluctuations, especially when cell density increased (Supplementary Fig. S1), requiring rapid change in cell metabolism and photosynthetic activity. In HL conditions, when cells were at the exponential phase, the light gradient experienced by cells was between 850 µmol m^{-2} s^{-1} and 390 µmol m^{-2} s^{-1}, thus even below

Published in : Journal of Experimental Botany (2023), vol. 74, n°15, pp. 4540-4558

DOI: 10.1093/jxb/erad170

Status : Postprint (Author's version)

the half-saturation intensity determined by the light curves reported in Fig. 2. In the experimental conditions applied here, HL adaptation is thus probably not driven mainly to prevent photooxidative stress but to exploit the higher light intensity available more efficiently. Accordingly, HL cells were more efficient than LL cells in using photosynthetically higher irradiances (Supplementary Fig. S3). The drawback of this adaptation is that HL cells were less efficient than LL cells at lower irradiances (Supplementary Fig. S3), demonstrating that acclimation to HL or LL conditions allows *C. vulgaris* to better use the light intensity available in that specific condition.

The reduced accumulation of Chl-binding proteins in *C. vulgaris* cells grown in HL is consistent with previous findings in the case of *C. reinhardtii* or *Synechocystis* sp. PCC 6803 (Toyoshima *et al.*, 2019). Moreover, a conserved feature between *C. reinhardtii*, *Synechocystis* sp. PCC 6803, and *C. vulgaris* acclimation to HL is the unchanged accumulation of carbonfixing enzymes on a protein basis, but while ATP synthase and NDH subunits were up-regulated in HL in *Synechocystis* sp. PCC 6803, this was not the case for *C. reinhardtii* (Toyoshima *et al.*, 2019) or *C. vulgaris* (this work), suggesting a peculiar adaptation in cyanobacteria, where photosynthetic electron transport and respiration share several electron carriers and ATP biosynthetic enzymes. For both *C. reinhardtii* and *C. vulgaris*, HL acclimation resulted in improved photosynthetic activity,

Published in : Journal of Experimental Botany (2023), vol. 74, n°15, pp. 4540-4558

DOI: 10.1093/jxb/erad170

Status : Postprint (Author's version)

with increased PSI activity, reduced saturation of the photosynthetic electron transport chain, and improved lightdependent oxygen evolution. The adaptation observed for the photosynthetic electron transport chain allows cells to properly use the higher availability of photons in HL, increasing the excitation pressure on PSI—which has a higher photochemical efficiency compared with PSII—and allows them to rapidly oxidize plastocyanin and consequently plastoquinones, the electron acceptors for PSII. Moreover, the contribution of PTOX in oxidizing plastoquinones was higher in HL cells, revealing chlororespiration as a strategy to desaturate the photosynthetic electron transport as previously reported in the case of the light-tolerant *Chlorella ohadii* (Kedem *et al.*, 2021). The increased solanesyl diphosphate synthase content suggests a key requirement for HL cells to have sufficient plastoquinone and ubiquinone availability as electron carriers. The consequences of these adaptations are evident from the light-dependent oxygen evolution curves of HL-grown cells, having an increased efficiency on a Chl basis of PSII in stripping electrons for water, releasing oxygen, and fueling the photosynthetic electron chain. It is interesting to note that a relative increase in cyclic electron transport could also be measured in HL-acclimated cells from ECS measurements, leading to a potential increase of the ATP/NADPH ratio for the ATP and NADPH produced in the light phase of photosynthesis. Despite the higher photosynthetic electron flow in HL cells, the ECS signals were similar in HL versus LL cells, demonstrating

Published in : Journal of Experimental Botany (2023), vol. 74, n°15, pp. 4540-4558

DOI: 10.1093/jxb/erad170

Status : Postprint (Author's version)

that increased proton pumping in the lumen—associated with increased electron transport—was rapidly used to produce ATP rather than to induce lumen acidification.

HL cells grew faster and reached a higher biomass concentration compared with *C. vulgaris* grown in LL. Increased biomass production in HL cells requires more CO_2 fixation, which is consistent with the increased photochemical activity leading to greater ATP and NADPH production (Fig. 6). Moreover, the content of Rubisco was increased in HL cells on a Chl basis (Supplementary Fig. S8), suggesting an increased capacity of carbon fixation enzymes to consume the products of the photosynthetic light phase. ATP consumption by CO_2 fixation reactions releases its precursor ADP, which can be used by thylakoidal ATP synthase, leading to efficient proton flux back to the stroma. Similarly, light-dependent NADPH consumption implies rapid regeneration of $NADP^+$ as an electron acceptor for photosynthetic electron transport. Consequently, upon light exposure, $NAD(P)H/NAD(P)^+$ quickly reaches a balanced pseudo-stationary phase only in HL cells, whereas the reduction of NADPH exceeds its oxidation in LL cells (Fig. 2), leading to reduced $NADP^+$ availability and increased risk of saturation of the photosynthetic electron transport chain.

Increased carbon fixation leads to greater carbon flow through the cell, with effects on metabolism (Fig. 6); mitochondrial activity was indeed affected by the light used for

Published in : Journal of Experimental Botany (2023), vol. 74, n°15, pp. 4540-4558

DOI: 10.1093/jxb/erad170

Status : Postprint (Author's version)

growth, with increased mitochondrial respiration observed in HL cells. In the case of LL cells, the light gradient to which cells were exposed (up to 70–30 µmol $m^{-2}s^{-1}$) is much closer to the light compensation point (22.59 µmol m^{-2} s^{-1}), leading to a major requirement for photosynthate to support cell metabolism and respiratory activity, reducing the carbon availability for biomass accumulation (Supplementary Fig. S2). According to the results obtained with specific inhibitors of the mitochondrial electron transport chain, the increased respiration in HL cells was mainly due to higher activity in the alternative electron transport pathway, which does not produce ATP but consumes reducing power. We can speculate that in HL cells, the higher carbon flow toward the mitochondria driven by increased carbon fixation induced an increased electron flow toward NADH or ubiquinones that must be oxidized to prevent unbalanced availability of oxidized cofactors. Accordingly, the proteomic analysis revealed that a succinate dehydrogenase enzyme involved in the TCA cycle that causes reduction of ubiquinone was up-regulated in HL cells. Moreover, the increased contribution of alternative respiratory pathways in HL conditions could be involved in dissipating chloroplast reducing power arriving in the mitochondria through the malate valve, by which malate is exported from the chloroplast to the cytosol and then oxidized in the mitochondria (Ocheretina *et al.*, 2000; Scheibe, 2004; Vishwakarma *et al.*, 2014): faster regeneration of $NADP^+$ in the chloroplast is indeed required to support increased thylakoidal electron

Published in : Journal of Experimental Botany (2023), vol. 74, n°15, pp. 4540-4558

DOI: 10.1093/jxb/erad170

Status : Postprint (Author's version)

transport in cells exposed to HL. The increased accumulation of an adenylate kinase predicted to be localized in the mitochondria suggests that a fraction of the ATP produced by the TCA cycle and oxidative phosphorylation is hydrolyzed to regenerate ADP. This is a different situation compared with the plastid, where excess ATP produced is rapidly consumed by carbon fixation reactions to regenerate ADP.

One of the adaptation mechanisms observed for acclimation to different light intensities observed in *C. vulgaris* shared with *C. reinhardtii* is the decrease in Chl content in HL cells (Table 1). Chl biosynthesis is strictly dependent on nitrogen assimilation; HL cells were characterized by reduced nitrate reductase expression with consequently reduced potential for nitrogen assimilation. However, nitrogen assimilation is required for ammonium production and amino acid biosynthesis. HL cells were indeed characterized by up-regulation of enzymes involved in the degradation of amino acids and amino acid transporters, suggesting amino acid catabolism as a strategy to recycle the amino groups in conditions where nitrogen assimilation is reduced to inhibit Chl biosynthesis. The reduced protein content per dry weight measured in HL cells (Supplementary Fig. S8) could be at least partially related to reduced content of Chl-binding proteins. It is interesting to note that among the enzymes involved in amino acid catabolism that were up-regulated in HL, we identified l-asparaginase, an enzyme used as a treatment for

Published in : Journal of Experimental Botany (2023), vol. 74, n°15, pp. 4540-4558

DOI: 10.1093/jxb/erad170

Status : Postprint (Author's version)

acute lymphoblastic leukemia. *Chlorella vulgaris* was suggested as a potential source of l-asparaginase (Ebrahiminezhad *et al.*, 2014); here we showed that HL acclimation increased production of this enzyme.

HL acclimation was previously demonstrated in *C. vulgaris* to increase the lipid fraction of the dry weight (Cecchin *et al.*, 2019). In line with this, our proteomic analysis revealed that HL cells had lower expression of a caleosin/peroxygenase 2-like protein, an enzyme involved in oil body degradation. No enzymes involved in lipid biosynthesis were up-regulated in HL, except for those involved in sterol biosynthesis. Increased sterol content was reported in different microalgae species exposed to high light (Randhir *et al.*, 2020). The specific role of sterols in microalgae has not been sufficiently investigated, but these molecules are reportedly involved in membrane fluidity, membrane-associated metabolic processes, and signal transduction. Understanding the possible increase in sterol biosynthesis in HL cells and its importance for HL acclimation requires further dedicated work. Considering the possible market opportunity for sterols produced by microalgae (Randhir *et al.*, 2020), the evaluation of the influence of irradiance of growth on the sterol production yield could pave the way for specific biotechnological applications.

Published in : Journal of Experimental Botany (2023), vol. 74, n°15, pp. 4540-4558

DOI: 10.1093/jxb/erad170

Status : Postprint (Author's version)

Acclimation to different irradiances implies the activation of cell signaling mechanisms controlling the activities of specific proteins and gene expression. Only two transcription factors were differentially expressed in HL versus LL cells of *C. vulgaris*. Identifying transcription factors by proteomic analysis is challenging due to their low abundance in protein extracts. However, the identification of g2204.t1 and g5610. t1 gene products up-regulated in LL and HL, respectively, suggests their major role controlling the gene expression patterns at these irradiances. A member of the heliorhodopsin protein family had one of the highest fold changes in HL, suggesting that photoreceptors may be involved in triggering cell adaptations to increased irradiances (Fig. 6). Moreover, subunit 6 of the COP9 signalosome was up-regulated in HL, and COP9 is a component of photoreceptor-mediated signaling in plants exposed to HL (Wei *et al.*, 1994; Chamovitz *et al.*, 1996). Other possible components of this signaling mechanism include a Gpr1-like protein, a GTPase-activating subunit (TBC domain-containing protein), and several kinases and phosphatases (Supplementary Table S4). It is intriguing that the aarF domain-containing kinases (g5742.t1, g9784.t1, and g7165.t1) were up-regulated in HL cells, since their homolog in *A. thaliana* (ABC1K1) was reported to be associated with plastoglobuli-triggering of plastoquinone and carotenoid biosynthesis (Martinis *et al.*, 2014).

Published in : Journal of Experimental Botany (2023), vol. 74, n°15, pp. 4540-4558

DOI: 10.1093/jxb/erad170

Status : Postprint (Author's version)

In conclusion, we clarified some specific mechanisms activated in *C. vulgaris* cells following long-term exposure to LL or HL. Photosynthetic activity was improved in HL conditions despite reductions in pigment content and light-harvesting properties. The increased energy availability in HL stimulates the photosynthetic apparatus to increase PTOX and PSI activity, allowing for more efficient desaturation of the photosynthetic electron transport chain. This, combined with increased carbon fixation and ADP and $NADP^+$ regeneration, enables cells to prevent saturation of the photosynthetic apparatus. The possible increase in carbon flow in HL cells is likely to be at the base of the enhanced mitochondrial respiration in this condition, mainly related to increased alternative oxidative pathway activity without ATP production. The ATP demand in HL conditions is probably sufficiently supplied by photosynthetic activity in the chloroplasts. The proteomic analysis results clarified which proteins are differentially expressed in LL versus HL, and the list included several enzymes involved in cell metabolism and intracellular transport. Moreover, several putative components of cell acclimation mechanisms were identified as differentially expressed, suggesting a major role for a heliorhodopsin homolog for cell response to different irradiances. It is worth noting that the increased AOX and PTOX activity in HL cells and the capacity to prevent over-reduction of $NAD(P)^+$ to NAD(P)H is a shared feature between HL-acclimated *C. vulgaris* and the extremely high light-tolerant *C. ohadii*, where this adaptations was even more

Published in : Journal of Experimental Botany (2023), vol. 74, n°15, pp. 4540-4558

DOI: 10.1093/jxb/erad170

Status : Postprint (Author's version)

evident (Treves *et al.*, 2020): the capacity to properly tune the redox state of mitochondria and chloroplasts is probably a key strategy to ensure survival and a high growth rate in HL conditions. The results described here suggest that a specific mutagenesis approach is required to elucidate the specific functions of the different proteins identified and clarify their possible roles in acclimation to different irradiances.

SUPPLEMENTARY DATA

The following supplementary data are available at *JXB* online. Dataset S1. Proteins identified by proteomic analysis of *Chlorella vulgaris* cells grown in HL or LL conditions.

Dataset S2. Differentially expressed proteins in HL- versus LL-acclimated *Chlorella vulgaris* cells.

Dataset S3. List of proteins identified by proteomic analysis involved in different metabolic pathways.

Table S1. PSII antenna size of *Chlorella vulgaris* cells acclimated to LL or HL.

Table S2. Differently expressed proteins annotated as peptidylprolyl isomerase.

Table S3. Differently expressed proteins involved in the light phase of photosynthesis.

Table S4. Differently expressed proteins in HL versus LL involved in transport and trafficking.

Published in : Journal of Experimental Botany (2023), vol. 74, n°15, pp. 4540-4558

DOI: 10.1093/jxb/erad170

Status : Postprint (Author's version)

Table S5. Differently expressed proteins in HL versus LL involved in cell signaling.

Fig. S1. Transmittance of the cell cultures and estimation of the light gradient in LL and HL conditions.

Fig. S2. Growth curves, growth rates, and dry weight of *Chlorella vulgaris* cells in LL and HL conditions.

Fig. S3. Light curves of LL- and HL-acclimated cells measured as net light-dependent oxygen evolution rates at different actinic lights normalized on a cell basis.

Fig. S4. PTOX activity in HL- and LL-acclimated *Chlorella vulgaris* cells.

Fig. S5. NPQ kinetics at different actinic lights.

Fig. S6. Protein content per cell and per dry weight in LL and HL conditions.

Fig. S7, REVIGO software visualization of all GO terms resulting upon GSEA.

Fig. S8. Western blot analysis of photosynthetic proteins.

Fig. S9. Alignment of the g7323.t1 gene product with heliorhodopsin proteins.

Fig. S10. Alignment of the g314.t1 gene product with URM1 protein encoded in the human genome.

Published in : Journal of Experimental Botany (2023), vol. 74, n°15, pp. 4540-4558

DOI: 10.1093/jxb/erad170

Status : Postprint (Author's version)

ACKNOWLEDGEMENTS

We would like to thank Yvan Eb-Levadoux and Catherine Nury for computational assistance and establishing the DIA proteomics workflow.

AUTHOR CONTRIBUTIONS

MB: conceptualization; MC, JS, LC, MH, LG, and SC: investigation; JS and MH: data curation; JS, MH, JH, NI, and BT: methodology; MB, CR, NI, and BT: supervision; MC, SC, and JS: visualization; MB: writing— original draft; MB, JS, MC, SC, CR, NI, and BT: writing— review and editing; MB and CR: funding acquisition.

CONFLICT OF INTEREST

JS, LC, MH, JH, NVI, and BT are employees of Philip Morris International.

FUNDING

Philip Morris International funded the proteomics investigations. The research was supported by the H2020 European Research Council Starting Grant SOLENALGAE (679814) to MB. CR acknowledges Fonds De La Recherche Scientifique FNRS-FWO EOS Project 30829584, FNRS CDR J.0175.20, and Action de Recherche Concertée from the University of Liege (DARKMET ARC grant 17/21-08).

Published in : Journal of Experimental Botany (2023), vol. 74, n°15, pp. 4540-4558

DOI: 10.1093/jxb/erad170

Status : Postprint (Author's version)

DATA AVAILABILITY

The mass spectrometry proteomics data have been deposited in the ProteomeXchange Consortium via the PRIDE partner repository with the dataset identifier PXD037846 (Perez-Riverol *et al.*, 2022).

Published in : Journal of Experimental Botany (2023), vol. 74, n°15, pp. 4540-4558

DOI: 10.1093/jxb/erad170

Status : Postprint (Author's version)

References

Afzal AJ, Wood AJ, Lightfoot DA. 2008. Plant receptor-like serine threonine kinases: roles in signaling and plant defense. Molecular Plant-Microbe Interactions **21**, 507–517.

Allen MM, Stanier RY. 1968. Growth and division of some unicellular blue-green algae. Journal of General Microbiology **51**, 199–202.

Allorent G, Tokutsu R, Roach T, *et al*. 2013. A dual strategy to cope with high light in *Chlamydomonas reinhardtii*. The Plant Cell **25**, 545–557.

Ananyev G, Gates C, Kaplan A, Dismukes GC. 2017. Photosystem II-cyclic electron flow powers exceptional photoprotection and record growth in the microalga *Chlorella ohadii*. Biochimica et Biophysica Acta **1858**, 873–883.

Arnon DI, Tsujimoto HY, Tang GMS. 1981. Proton transport in photooxidation of water: a new perspective on photosynthesis. Proceedings of the National Academy of Sciences, USA **78**, 2942–2946.

Arriola M, Velmurugan N, Zhang Y, Plunkett M, Hondzo H, Barney B. 2018. Genome sequences of *Chlorella sorokiniana* UTEX 1602 and *Micractinium conductrix* SAG 241.80: implications to maltose excretion by a green alga. The Plant Journal **93**, 566–586.

Bailleul B, Berne N, Murik O, *et al*. 2015. Energetic coupling between plastids and mitochondria drives CO_2 assimilation in diatoms. Nature **524**, 366–369.

Published in : Journal of Experimental Botany (2023), vol. 74, n°15, pp. 4540-4558

DOI: 10.1093/jxb/erad170

Status : Postprint (Author's version)

Baker NR. 2008. Chlorophyll fluorescence: a probe of photosynthesis in vivo. Annual Review of Plant Biology **59**, 89–113.

Ballottari M, Dall'Osto L, Morosinotto T, Bassi R. 2007. Contrasting behavior of higher plant photosystem I and II antenna systems during acclimation. Journal of Biological Chemistry **282**, 8947–8958.

Barth E, Hübler R, Baniahmad A, Marz M. 2016. The evolution of COP9 signalosome in unicellular and multicellular organisms. Genome Biology and Evolution **8**, 1279–1289.

Bennoun P. 1982. Evidence for a respiratory chain in the chloroplast. Proceedings of the National Academy of Sciences, USA **79**, 4352–4356.

Bernaerts T, Gheysen L, Foubert I, Hendrickx M, Van Loey A. 2019. The potential of microalgae and their biopolymers as structuring ingredients in food: a review. Biotechnology Advances **37**, 107419.

Blanc G, Duncan G, Agarkova I, *et al*. 2010. The Chlorella variabilis NC64A genome reveals adaptation to photosymbiosis, coevolution with viruses, and cryptic sex. The Plant Cell **22**, 2943–2955.

Boekema E, Braun H. 2007. Supramolecular structure of the mitochondrial oxidative phosphorylation system. Journal of Biological Chemistry **282**, 1–4.

Published in : Journal of Experimental Botany (2023), vol. 74, n°15, pp. 4540-4558

DOI: 10.1093/jxb/erad170

Status : Postprint (Author's version)

Bohrer AS, Kopriva S, Takahashi H. 2014. Plastid–cytosol partitioning and integration of metabolic pathways for APS/PAPS biosynthesis in *Arabidopsis thaliana*. Frontiers in Plant Science **5**, 751.

Bonente G, Ballottari M, Truong TB, Morosinotto T, Ahn TK, Fleming GR, Niyogi KK, Bassi R. 2011. Analysis of LhcSR3, a protein essential for feedback de-excitation in the green alga *Chlamydomonas reinhardtii*. PLoS Biology **9**, e1000577.

Bonente G, Pippa S, Castellano S, Bassi R, Ballottari M. 2012. Acclimation of *Chlamydomonas reinhardtii* to different growth irradiances. Journal of Biological Chemistry **287**, 5833–5847.

Burlacot A, Peltier G, Li-Beisson Y. 2019. Subcellular energetics and carbon storage in *Chlamydomonas*. Cells **8**, 1154.

Camacho F, Macedo A, Malcata F. 2019. Potential industrial applications and commercialization of microalgae in the functional food and feed industries: a short review. Marine Drugs **17**, 312.

Cardol P, De Paepe R, Franck F, Forti G, Finazzi G. 2010. The onset of NPQ and Deltamu(H)+ upon illumination of tobacco plants studied through the influence of mitochondrial electron transport. Biochimica et Biophysica Acta **1797**, 177–188.

Cecchin M, Jeong J, Son W, *et al.* 2021a. LPA2 protein is involved in photosystem II assembly in *Chlamydomonas reinhardtii*. The Plant Journal **107**, 1648–1662.

Published in : Journal of Experimental Botany (2023), vol. 74, n°15, pp. 4540-4558

DOI: 10.1093/jxb/erad170

Status : Postprint (Author's version)

Cecchin M, Marcolungo L, Rossato M, Girolomoni L, Cosentino E, Cuine S, Li-Beisson Y, Delledonne M, Ballottari M. 2019. *Chlorella vulgaris* genome assembly and annotation reveals the molecular basis for metabolic acclimation to high light conditions. The Plant Journal **100**, 1289–1305.

Cecchin M, Paloschi M, Busnardo G, Cazzaniga S, Cuine S, Li-Beisson Y, Wobbe L, Ballottari M. 2021b. CO_2 supply modulates lipid remodelling, photosynthetic and respiratory activities in *Chlorella* species. Plant, Cell & Environment **44**, 2987–3001.

Chamovitz DA, Wei N, Osterlund MT, von Arnim AG, Staub JM, Matsui M, Deng XW. 1996. The COP9 complex, a novel multisubunit nuclear regulator involved in light control of a plant developmental switch. Cell **86**, 115–121.

Chazan A, Rozenberg A, Mannen K, Nagata T, Tahan R, Yaish S, Larom S, Inoue K, Béjà O, Pushkarev A. 2022. Diverse heliorhodopsins detected via functional metagenomics in freshwater Actinobacteria, Chloroflexi and Archaea. Environmental Microbiology **24**, 110–121.

Chisti Y. 2008. Biodiesel from microalgae beats bioethanol. Trends in Biotechnology **26**, 126–131.

Chukhutsina VU, Fristedt R, Morosinotto T, Croce R. 2017. Photoprotection strategies of the alga *Nannochloropsis gaditana*. Biochimica et Biophysica Acta **1858**, 544–552.

Published in : Journal of Experimental Botany (2023), vol. 74, n°15, pp. 4540-4558

DOI: 10.1093/jxb/erad170

Status : Postprint (Author's version)

Dang KV, Plet J, Tolleter D, *et al*. 2014. Combined increases in mitochondrial cooperation and oxygen photoreduction compensate for deficiency in cyclic electron flow in *Chlamydomonas reinhardtii*. The Plant Cell **26**, 3036–3050.

De Smet I, Voss U, Jürgens G, Beeckman T. 2009. Receptor-like kinases shape the plant. Nature Cell Biology **11**, 1166–1173.

Ebrahiminezhad A, Rasoul-Amini S, Ghoshoon MB, Ghasemi Y. 2014. *Chlorella vulgaris*, a novel microalgal source for L-asparaginase production. Biocatalysis and Agricultural Biotechnology **3**, 214–217.

Finazzi G, Rappaport F, Furia A, Fleischmann M, Rochaix JD, Zito F, Forti G. 2002. Involvement of state transitions in the switch between linear and cyclic electron flow in *Chlamydomonas reinhardtii*. EMBO Reports **3**, 280–285.

Fleischmann MM, Ravanel S, Delosme R, Olive J, Zito F, Wollman FA, Rochaix JD. 1999. Isolation and characterization of photoautotrophic mutants of *Chlamydomonas reinhardtii* deficient in state transition. Journal of Biological Chemistry **274**, 30987–30994.

Gentleman RC, Carey VJ, Bates DM, *et al*. 2004. Bioconductor: open software development for computational biology and bioinformatics. Genome Biology **5**, R80.

Girolomoni L, Bellamoli F, Valbuena G, Perozeni F, D'Andrea C, Cerullo G, Cazzaniga S, Ballottari M. 2020. Evolutionary divergence of photoprotection in the green algal lineage: a plant-

Published in : Journal of Experimental Botany (2023), vol. 74, n°15, pp. 4540-4558

DOI: 10.1093/jxb/erad170

Status : Postprint (Author's version)

like violaxanthin de-epoxidase enzyme activates the xanthophyll cycle in the green alga *Chlorella vulgaris* modulating photoprotection. New Phytologist **228**, 136–150.

Goehring AS, Rivers DM, Sprague GF. 2003. Urmylation: a ubiquitinlike pathway that functions during invasive growth and budding in yeast. Molecular Biology of the Cell **14**, 4329–4341.

González-Ballester D, Camargo A, Fernández E. 2004. Ammonium transporter genes in *Chlamydomonas*: the nitrate-specific regulatory gene Nit2 is involved in Amt1;1 expression. Plant Molecular Biology **56**, 863–878.

Gordillo FJ, Jiménez C, Chavarría J, Xavier Niell F. 2001. Photosynthetic acclimation to photon irradiance and its relation to chlorophyll fluorescence and carbon assimilation in the halotolerant green alga *Dunaliella viridis*. Photosynthesis Research **68**, 225–235.

Guarnieri MT, Nag A, Yang S, Pienkos PT. 2013. Proteomic analysis of *Chlorella vulgaris*: potential targets for enhanced lipid accumulation. Journal of Proteomics **93**, 245–253.

Houille-Vernes L, Rappaport F, Wollman FA, Alric J, Johnson X. 2011. Plastid terminal oxidase 2 (PTOX2) is the major oxidase involved in chlororespiration in *Chlamydomonas*. Proceedings of the National Academy of Sciences, USA **108**, 20820–20825.

Johnson X, Alric J. 2013. Central carbon metabolism and electron transport in *Chlamydomonas reinhardtii*: metabolic constraints for carbon partitioning between oil and starch. Eukaryotic Cell **12**, 776–793.

Published in : Journal of Experimental Botany (2023), vol. 74, n°15, pp. 4540-4558

DOI: 10.1093/jxb/erad170

Status : Postprint (Author's version)

Juneja A, Chaplen F, Murthy G. 2016. Genome scale metabolic reconstruction of *Chlorella variabilis* for exploring its metabolic potential for biofuels. Bioresource Technology **213**, 103–110.

Kedem I, Milrad Y, Kaplan A, Yacoby I. 2021. Juggling lightning: how *Chlorella ohadii* handles extreme energy inputs without damage. Photosynthesis Research **147**, 329–344.

Klein M, Papenbrock J. 2004. The multi-protein family of Arabidopsis sulphotransferases and their relatives in other plant species. Journal of Experimental Botany **55**, 1809–1820.

Kovalev K, Volkov D, Astashkin R, *et al*. 2020. High-resolution structural insights into the heliorhodopsin family. Proceedings of the National Academy of Sciences, USA **117**, 4131–4141.

Koyande A, Chew K, Rambabu K, Tao Y, Chu D, Show P. 2019. Microalgae: a potential alternative to health supplementation for humans. Food Science and Human Wellness **8**, 16–24.

Kuhlgert S, Austic G, Zegarac R, *et al*. 2016. MultispeQ Beta: a tool for large-scale plant phenotyping connected to the open PhotosynQ network. Royal Society Open Science **3**, 160592.

Lange PR, Geserick C, Tischendorf G, Zrenner R. 2008. Functions of chloroplastic adenylate kinases in Arabidopsis. Plant Physiology **146**, 492–504. **Lavaud J, Rousseau B, Etienne A.** 2004. General features of photoprotection by energy dissipation in planktonic diatoms (Bacillariophyceae). Journal of Phycology **40**, 130–137.

Lea US, Leydecker MT, Quilleré I, Meyer C, Lillo C. 2006. Posttranslational regulation of nitrate reductase strongly affects the levels of free amino acids and nitrate, whereas transcriptional regulation has only minor influence. Plant Physiology **140**, 1085–1094.

Published in : Journal of Experimental Botany (2023), vol. 74, n°15, pp. 4540-4558

DOI: 10.1093/jxb/erad170

Status : Postprint (Author's version)

Lemeille S, Turkina MV, Vener AV, Rochaix JD. 2010. Stt7-dependent phosphorylation during state transitions in the green alga *Chlamydomonas reinhardtii*. Molecular & Cellular Proteomics **9**, 1281–1295.

Lepetit B, Sturm S, Rogato A, Gruber A, Sachse M, Falciatore A, Kroth P, Lavaud J. 2012. High light acclimation in the secondary plastids containing diatom *Phaeodactylum tricornutum* is triggered by the redox state of the plastoquinone pool. Plant Physiology **161**, 853–865.

Li Y, Sommerfeld M, Chen F, Hu Q. 2010. Effect of photon flux densities on regulation of carotenogenesis and cell viability of *Haematococcus pluvialis* (Chlorophyceae). Journal of Applied Phycology **22**, 253–263.

Lin M, Oliver DJ. 2008. The role of acetyl-coenzyme A synthetase in Arabidopsis. Plant Physiology **147**, 1822–1829.

Lum KK, Kim J, Lei XG. 2013. Dual potential of microalgae as a sustainable biofuel feedstock and animal feed. Journal of Animal Science and Biotechnology **4**, 53.

Malkin S, Armond PA, Mooney HA, Fork DC. 1981. Photosystem II photosynthetic unit sizes from fluorescence induction in leaves: correlation to photosynthetic capacity. Plant Physiology **67**, 570–579.

Martinis J, Glauser G, Valimareanu S, Stettler M, Zeeman SC, Yamamoto H, Shikanai T, Kessler F. 2014. ABC1K1/PGR6 kinase: a regulatory link between photosynthetic activity and chloroplast metabolism. The Plant Journal **77**, 269–283.

Published in : Journal of Experimental Botany (2023), vol. 74, n°15, pp. 4540-4558

DOI: 10.1093/jxb/erad170

Status : Postprint (Author's version)

Mayr SJ, Mendel RR, Schwarz G. 2021. Molybdenum cofactor biology, evolution and deficiency. Biochimica et Biophysica Acta **1868**, 118883.

Nakai Y, Harada A, Hashiguchi Y, Nakai M, Hayashi H. 2012. Arabidopsis molybdopterin biosynthesis protein Cnx5 collaborates with the ubiquitin-like protein Urm11 in the thio-modification of tRNA. Journal of Biological Chemistry **287**, 30874–30884.

Nawrocki WJ, Santabarbara S, Mosebach L, Wollman FA, Rappaport F. 2016. State transitions redistribute rather than dissipate energy between the two photosystems in *Chlamydomonas*. Nature Plants **2**, 16031.

Niccolai A, Zittelli G, Rodolfi L, Biondi N, Tredici M. 2019. Microalgae of interest as food source: biochemical composition and digestibility. Algal Research **42**, 101617.

Nimmy MS, Kumar V, Suthanthiram B, Subbaraya U, Nagar R, Bharadwaj C, Jain PK, Krishnamurthy P. 2022. A systematic phylogenomic classification of the multidrug and toxic compound extrusion transporter gene family in plants. Frontiers in Plant Science **13**, 774885.

Niyogi KK. 2000. Safety valves for photosynthesis. Current Opinion in Plant Biology **3**, 455–460.

Ocheretina O, Haferkamp I, Tellioglu H, Scheibe R. 2000. Lightmodulated NADP-malate dehydrogenases from mossfern and green algae: insights into evolution of the enzyme's regulation. Gene **258**, 147–154.

Published in : Journal of Experimental Botany (2023), vol. 74, n°15, pp. 4540-4558

DOI: 10.1093/jxb/erad170

Status : Postprint (Author's version)

Ohara K, Sasaki K, Yazaki K. 2010. Two solanesyl diphosphate synthases with different subcellular localizations and their respective physiological roles in *Oryza sativa*. Journal of Experimental Botany **61**, 2683–2692.

Pan X, Eathiraj S, Munson M, Lambright DG. 2006. TBC-domain GAPs for Rab GTPases accelerate GTP hydrolysis by a dual-finger mechanism. Nature **442**, 303–306.

Peers G, Truong TB, Ostendorf E, Busch A, Elrad D, Grossman AR, Hippler M, Niyogi KK. 2009. An ancient light-harvesting protein is critical for the regulation of algal photosynthesis. Nature **462**, 518–521.

Perez-Riverol Y, Bai J, Bandla C, *et al*. 2022. The PRIDE database resources in 2022: a hub for mass spectrometry-based proteomics evidences. Nucleic Acids Research **50**, D543–D552.

Perozeni F, Cazzaniga S, Baier T, Zanoni F, Zoccatelli G, Lauersen K, Wobbe L, Ballottari M. 2020. Turning a green alga red: engineering astaxanthin biosynthesis by intragenic pseudogene revival in *Chlamydomonas reinhardtii*. Plant Biotechnology Journal **18**, 2053–2067.

Pushkarev A, Inoue K, Larom S, *et al*. 2018. A distinct abundant group of microbial rhodopsins discovered using functional metagenomics. Nature **558**, 595–599.

Rahman F, Hassan M, Rosli R, Almousally I, Hanano A, Murphy DJ. 2018. Evolutionary and genomic analysis of the caleosin/peroxygenase (CLO/PXG) gene/protein families in the Viridiplantae. PLoS One **13**, e0196669.

Published in : Journal of Experimental Botany (2023), vol. 74, n°15, pp. 4540-4558

DOI: 10.1093/jxb/erad170

Status : Postprint (Author's version)

Randhir A, Laird D, Maker G, Trengove R, Moheimani N. 2020. Microalgae: a potential sustainable commercial source of sterols. Algal Research **46**, 101772.

Rani A, Saini KC, Bast F, Mehariya S, Bhatia SK, Lavecchia R, Zuorro A. 2021. Microorganisms: a potential source of bioactive molecules for antioxidant applications. Molecules **26**, 1142.

Roberts J, Aubert S, Gout E, Bligny R, Douce R. 1997. Cooperation and competition between adenylate kinase, nucleoside diphosphokinase, electron transport, and ATP synthase in plant mitochondria studied by 31P-Nuclear magnetic resonance. Plant Physiology **113**, 191–199.

Rosch C, Rossmann M, Weickert S. 2019. Microalgae for integrated food and fuel production. Global Change Biology Bioenergy **11**, 326–334.

Rumeau D, Peltier G, Cournac L. 2007. Chlororespiration and cyclic electron flow around PSI during photosynthesis and plant stress response. Plant, Cell & Environment **30**, 1041–1051.

Sanz-Luque E, Chamizo-Ampudia A, Llamas A, Galvan A, Fernandez E. 2015. Understanding nitrate assimilation and its regulation in microalgae. Frontiers in Plant Science **6**, 899.

Sarayloo E, Tardu M, Unlu Y, Simsek S, Cevahir G, Erkey C, Kavakli I. 2017. Understanding lipid metabolism in high-lipid-producing *Chlorella vulgaris* mutants at the genome-wide level. Algal Research **28**, 244–252.

Sathasivam R, Radhakrishnan R, Hashem A, Abd Allah E. 2019. Microalgae metabolites: a rich source for food and medicine. Saudi Journal of Biological Sciences **26**, 709–722.

Published in : Journal of Experimental Botany (2023), vol. 74, n°15, pp. 4540-4558

DOI: 10.1093/jxb/erad170

Status : Postprint (Author's version)

Scheibe R. 2004. Malate valves to balance cellular energy supply. Physiologia Plantarum **120**, 21–26.

Schmitz J, Chowdhury MM, Hänzelmann P, Nimtz M, Lee EY, Schindelin H, Leimkühler S. 2008. The sulfurtransferase activity of Uba4 presents a link between ubiquitin-like protein conjugation and activation of sulfur carrier proteins. Biochemistry **47**, 6479–6489.

Schneider A, Steinberger I, Strissel H, *et al.* 2014. The Arabidopsis Tellurite resistance C protein together with ALB3 is involved in photosystem II protein synthesis. The Plant Journal **78**, 344–356.

Schreiber U, Klughammer C. 2009. New NADPH/9-AA module for the DUAL-PAM-100: description, operation and examples of application. PAM application Notes **2**, 1–13.

Serra-Maia R, Bernard O, Goncalves A, Bensalem S, Lopes F. 2016. Influence of temperature on *Chlorella vulgaris* growth and mortality rates in a photobioreactor. Algal Research **18**, 352–359.

Shahbazi M, Gilbert M, Labouré A-M, Kuntz M. 2007. Dual role of the plastid terminal oxidase in tomato. Plant Physiology **145**, 691–702.

Simicevic J, Deplancke B. 2017. Transcription factor proteomics—tools, applications, and challenges. Proteomics **17**, 1600317.

Simicevic J, Schmid AW, Gilardoni PA, *et al.* 2013. Absolute quantification of transcription factors during cellular differentiation using multiplexed targeted proteomics. Nature Methods **10**, 570–576.

Published in : Journal of Experimental Botany (2023), vol. 74, n°15, pp. 4540-4558

DOI: 10.1093/jxb/erad170

Status : Postprint (Author's version)

Simionato D, Sforza E, Corteggiani Carpinelli E, Bertucco A, Giacometti GM, Morosinotto T. 2011. Acclimation of *Nannochloropsis gaditana* to different illumination regimes: effects on lipids accumulation. Bioresource Technology **102**, 6026–6032.

Smith BM, Morrissey PJ, Guenther JE, Nemson JA, Harrison MA, Allen JF, Melis A. 1990. Response of the photosynthetic apparatus in *Dunaliella salina* (green algae) to irradiance stress. Plant Physiology **93**, 1433–1440.

Spaniol B, Lang J, Venn B, *et al*. 2022. Complexome profiling on the *Chlamydomonas lpa2* mutant reveals insights into PSII biogenesis and new PSII associated proteins. Journal of Experimental Botany **73**, 245–262.

Stitt M, Lilley RM, Heldt HW. 1982. Adenine nucleotide levels in the cytosol, chloroplasts, and mitochondria of wheat leaf protoplasts. Plant Physiology **70**, 971–977.

Supek F, Bošnjak M, Škunca N, Šmuc T. 2011. REVIGO summarizes and visualizes long lists of gene ontology terms. PLoS One **6**, e21800.

Tardif M, Atteia A, Specht M, *et al*. 2012. PredAlgo: a new subcellular localization prediction tool dedicated to green algae. Molecular Biology and Evolution **29**, 3625–3639.

Toyoshima M, Sakata M, Ohnishi K, Tokumaru Y, Kato Y, Tokutsu R, Sakamoto W, Minagawa J, Matsuda F, Shimizu H. 2019. Targeted proteome analysis of microalgae under high-light conditions by optimized protein extraction of photosynthetic organisms. Journal of Bioscience and Bioengineering **127**, 394–402.

Published in : Journal of Experimental Botany (2023), vol. 74, n°15, pp. 4540-4558

DOI: 10.1093/jxb/erad170

Status : Postprint (Author's version)

Treves H, Raanan H, Kedem I, *et al*. 2016. The mechanisms whereby the green alga *Chlorella ohadii*, isolated from desert soil crust, exhibits unparalleled photodamage resistance. New Phytologist **210**, 1229–1243.

Treves H, Siemiatkowska B, Luzarowska U, *et al*. 2020. Multi-omics reveals mechanisms of total resistance to extreme illumination of a desert alga. Nature Plants **6**, 1031–1043.

Uhmeyer A, Cecchin M, Ballottari M, Wobbe L. 2017. Impaired mitochondrial transcription termination disrupts the stromal redox poise in *Chlamydomonas*. Plant Physiology **174**, 1399–1419.

Vanlerberghe G. 2013. Alternative oxidase: a mitochondrial respiratory pathway to maintain metabolic and signaling homeostasis during abiotic and biotic stress in plants. International Journal of Molecular Sciences **14**, 6805–6847.

Väremo L, Nielsen J, Nookaew I. 2013. Enriching the gene set analysis of genome-wide data by incorporating directionality of gene expression and combining statistical hypotheses and methods. Nucleic Acids Research **41**, 4378–4391.

Vecchi V, Barera S, Bassi R, Dall'Osto L. 2020. Potential and challenges of improving photosynthesis in algae. Plants (Basel) **9**, 67.

Vishwakarma A, Bashyam L, Senthilkumaran B, Scheibe R, Padmasree K. 2014. Physiological role of AOX1a in photosynthesis and maintenance of cellular redox homeostasis under high light in *Arabidopsis thaliana*. Plant Physiology and Biochemistry **81**, 44–53.

Published in : Journal of Experimental Botany (2023), vol. 74, n°15, pp. 4540-4558

DOI: 10.1093/jxb/erad170

Status : Postprint (Author's version)

Wakao S, Shih PM, Guan K, *et al*. 2021. Discovery of photosynthesis genes through whole-genome sequencing of acetate-requiring mutants of *Chlamydomonas reinhardtii*. PLoS Genetics **17**, e1009725.

Wang Y, Stessman D, Spalding M. 2015. The CO_2 concentrating mechanism and photosynthetic carbon assimilation in limiting CO_2: how Chlamydomonas works against the gradient. The Plant Journal **82**, 429–448.

Wei N, Chamovitz DA, Deng XW. 1994. Arabidopsis COP9 is a component of a novel signaling complex mediating light control of development. Cell **78**, 117–124.

Yamano T, Miura K, Fukuzawa H. 2008. Expression analysis of genes associated with the induction of the carbon-concentrating mechanism in *Chlamydomonas reinhardtii*. Plant Physiology **147**, 340–354.

Yang W, Catalanotti C, D'Adamo S, *et al*. 2014. Alternative acetate production pathways in *Chlamydomonas reinhardtii* during dark anoxia and the dominant role of chloroplasts in fermentative acetate production. The Plant Cell **26**, 4499–4518.

Zhu SH, Green BR. 2010. Photoprotection in the diatom *Thalassiosira pseudonana*: role of LI818-like proteins in response to high light stress. Biochimica et Biophysica Acta **1797**, 1449–1457.

Published in : Journal of Experimental Botany (2023), vol. 74, n°15, pp. 4540-4558

DOI: 10.1093/jxb/erad170

Status : Postprint (Author's version)

Zuniga C, Li C, Huelsman T, *et al*. 2016. Genome-scale metabolic model for the green alga *Chlorella vulgaris* UTEX 395 accurately predicts phenotypes under autotrophic, heterotrophic, and mixotrophic growth conditions. Plant Physiology **172**, 589–602.